Ultraviolet Radiation and Bio-optics in Crater Lake, Oregon

B. R. Hargreaves[1], S. F. Girdner[2], M. W. Buktenica[2], R. W.Collier[3],

E. Urbach[4], G. L. Larson[5]

Submission date: 7 July 2005
(edit version 11/18/2005, 11/20/2005, 5/12/06 BRH)

[1] Department of Earth & Environmental Sciences, 31 Williams Drive, Lehigh University, Bethlehem, PA 18015 (brh0@lehigh.edu, 610-758-3683)

[2] Crater Lake National Park, Crater Lake, OR 97604

[3] Oregon State University, COAS, 104 Ocean. Admin. Bldg. Corvallis, OR 97331.

[4] Department of Microbiology, Oregon State University, 220 Nash Hall, Corvallis, OR 97331

Current address: eMetagen, L.L.C., 3591 Anderson St., Suite 207, Madison, WI 53704

[5] USGS Forest and Rangeland Ecosystem Science Center, 3200 Jefferson Way, Corvallis, OR 97331

This paper has not been submitted elsewhere in identical or similar form, nor will it be during the first three months after its submission to *Hydrobiologia*.

Key words: ultraviolet radiation, plankton, optics, UV-B, stratospheric ozone

ABSTRACT

Crater Lake, Oregon, is a mid-latitude caldera lake famous for its depth (594 m) and blue color. Recent underwater spectral measurements of solar radiation (310–800 nm) support earlier observations of unusual transparency and extend these to UV-B wavelengths. New data suggest that penetration of solar UVR into Crater Lake has a significant ecological impact. Evidence includes a correlation between water column chlorophyll-a and stratospheric ozone since 1984, the scarcity of organisms in the upper water column, and apparent UV screening pigments in phytoplankton that vary with depth. The lowest UV-B diffuse attenuation coefficients ($K_{d,320}$) were similar to those reported for the clearest natural waters elsewhere, and were lower than estimates for pure water published in 1981. Optical proxies for UVR attenuation were correlated with chlorophyll-a concentration (0–30 m) during typical dry summer months from 1984–2002. Using all proxies and measurements of UV transparency, decadal and longer cycles were apparent but no long-term trend since the first optical measurement in 1896.

INTRODUCTION

Current interest in ultraviolet radiation (UVR) in Crater Lake, Oregon, follows naturally from its well-known transparency (Larson, 2002) and the greater incident UVR and lake transparency found at high elevations (Laurion et al., 2000; Sommaruga, 2001). Crater Lake is famous for its depth (594 m, Bacon et al., 2002), visual clarity, and deep blue color. It is sub-alpine in elevation at 1800 m yet it rarely freezes during winter; it has an average radius of 4.1 km and is enclosed by a volcano's caldera, whose steep walls shelter it from strong winds and limit hydraulic exchange largely to snowmelt, direct precipitation, evaporation, and outseepage (Redmond, 1999). Optical studies of water transparency in Crater Lake began in 1896 when a white dinner plate was lowered into the water until it disappeared at 30 m (Diller, 1897, cited in Larson et al., 1996a). Black and white Secchi disk measurements were made sporadically since then until the late 1970s, when regular measurements began. An underwater photometer equipped with colored filters and matching deck cell was used to characterize water transparency in 1940 (Utterback et al., 1942) and again in the late 1960s (Larson et al., 1996a; Larson, 2002). Concerns about pollution and degraded water quality in the 1970s led to an improved sewage disposal at the tourist facilities in 1975 and the complete removal of sewage in 1991 (Larson 2002), and to a federally funded monitoring program beginning in 1983 (Larson et al., 1996a; Larson, 2002). Routine optical measurements with modern instruments began in 1987 with a beam transmissometer (25 cm, 660 nm beam) attached to an automated CTD profiler (conductivity, temperature, depth); a UV scanning radiometer was added in 1996, and a chlorophyll fluorescence sensor was added in 1999.

Crater Lake is not only visually clear; it is also remarkably transparent to solar UVR (280–400 nm). In the 1930s Crater Lake water was examined to determine scattering of UVR in a

laboratory comparison with purified water and deep ocean water (Pettit, 1936), only a decade after the first measurements of solar ultraviolet radiation (UVR) in the atmosphere using a photoelectric sensor (Coblentz & Stair, 1936), and more than a decade before the penetration of solar UV-B radiation (280–320 nm) into natural waters was reported using a photoelectric sensor (Johnson [Jerlov], 1946; Jerlov 1950; Højerslev 1994). Crater Lake underwater UVR was first investigated in the 1960s. Tests of newly designed scanning underwater radiometers were the basis for a series of summer measurements in Crater Lake during 1964–69 (Tyler 1965; Smith & Tyler, 1967; Tyler & Smith, 1970; Smith et al., 1973). Spectral measurements from 1969 in Crater Lake were also compared with similar measurements in Lake Tahoe, another clear deep lake (Smith et al., 1973). These authors and Pettit (1936) observed similarities between the upper 20 m of Crater Lake water and highly purified water and noted the importance of scattering of short wavelengths to the color of Crater Lake. In an effort to characterize spectral absorption and attenuation by pure water from data published to date, Smith and colleagues used the 1967 Crater Lake optical measurements (360–700 nm) as the basis for equating its transparency to the clearest waters of the Sargasso Sea (Smith & Tyler, 1976) and established absorption and attenuation spectra (200–800 nm) for pure freshwater and seawater that would be used for many years (Smith & Baker, 1981). Morel & Prieur (1977) used Crater Lake reflectance data in an assessment of scattering and absorption in both pure and natural waters to infer the content of ocean water by remote sensing.

The high elevation (1800 m) and frequently clear summer skies combine with the UV transparent water and shallow upper mixed layer (usually < 10 m deep and persistent from summer through early fall, Larson et al., 1996a) to create an unusually broad and stable depth gradient of UVR exposure for aquatic organisms. Research on underwater UVR and its potential

for biological impact has increased in response to concerns about depletion of stratospheric ozone and climate change (Schindler & Curtis 1997; Pienitz & Vincent, 2000). Several reports on the distribution of organisms in Crater Lake suggest a possible inhibitory role for UVR (McIntire et al., 1994; McIntire et al., 1996; Larson et al., 1996b), especially above 40 m. UVR measurements in Crater Lake resumed in 1996 when a submersible wavelength-scanning radiometer (300–800 nm) was added to the monitoring program and used to acquire incident and underwater solar spectra at a range of depths. Visiting scientists made additional optical measurements in UV and visible wavelengths starting in 1999. A recent report confirmed the unusual UV-B transparency of Crater Lake and derived estimates of UV-B attenuation by pure water and phytoplankton from measurements in its surface waters (Hargreaves, 2003).

Our approach here was first to characterize the spectral properties of near-surface and deeper water in Crater Lake, emphasizing UVR wavelengths, and to compare these with other clear lakes and ocean waters. We then used bio-optical signals and daily stratospheric ozone levels to examine factors controlling UVR attenuation with depth and over time, to develop proxies for estimating UVR attenuation, and to evaluate the impact of UVR on the Crater Lake ecosystem. Finally, we used the complete record of direct measurements and proxy estimates of UVR attenuation to look at long-term trends, and to speculate about the impact of future climate change.

OPTICAL BACKGROUND

In studies of underwater light in aquatic ecosystems it is customary to characterize the transparency or attenuation of natural waters instead of underwater irradiance because transparency and attenuation are persistent properties from which underwater UVR irradiance can be calculated for any given time and depth. A useful measure of UVR transparency in

natural waters is $K_{d,\lambda}$, the spectral diffuse attenuation coefficient for downwelling irradiance $E_{d,\lambda}$ (Baker & Smith, 1979). K_d can be used to characterize water transparency and factors controlling transparency or to reconstruct underwater solar spectra as a function of depth. K_d is calculated either from discrete measurements of E_d made at several depths or from a set of E_d values recorded over a continuous range of depths. An average K_d is often calculated for a range of depths considered to be optically mixed (e.g. the upper mixed layer or epilimnion) but depth-specific K_d values can also be derived from underwater measurements to reveal how attenuation varies with depth.

Valid spectral applications of K_d values are difficult to obtain unless the wavebands are narrow enough to be "spectrally-neutral" (where $K_{d,\lambda}$ varies little across the waveband). An example of a broad yet spectrally-neutral waveband in clear water is 400–500 nm. In contrast, when underwater K_d is calculated in clear water for the PAR (400–700 nm, PAR = photosynthetically active radiation) waveband, attenuation of solar radiation varies strongly with depth even though the water is uniformly mixed (Kirk, 1994b). This is because spectral variation in $K_{d,\lambda}$ leads to shifts with depth in relative proportions of different wavelengths within the waveband. $K_{d,PAR}$ in a uniformly-mixed body of clear water is much greater at the surface than it is deeper because at the surface the strongly attenuated red part of the solar spectrum contributes to the average K_d; at deeper depths only the weakly attenuated blue and violet wavelengths are still present and only these contribute to average K_d. Another example of a problematic broadband application is when the entire UV-B range of wavelengths is used to calculate a single $K_{d,UVB}$, yielding values that are difficult to compare or interpret (Hargreaves, 2003). Underwater spectral radiometers useful for K_d determinations have moderate bandwidths in the range of 10

nm or less (Kirk et al., 1994), although significant spectral shifts can occur with moderate bandwidth sensors at the shorter UV-B wavelengths (Patterson et al., 1997).

Other sensor properties can influence spectral K_d measurements. For downwelling irradiance (E_d) a sensor with an accurate cosine response to the angle of incident photons is needed. Accurate determinations of $K_{d,\lambda}$ are possible when a sensor is not accurately calibrated as long as the same sensor is used in all measurements, travels in a vertical plane during displacement over precisely determined depths, and maintains stability of its wavelength sensitivity, calibration, and cosine response to the angular distribution of light. In practice a correction for a dark offset signal and response to changing temperature may need to be incorporated into the measurement protocol (Kirk et al., 1994). Internal radiation sources (fluorescence and Raman scattering, also called "inelastic scattering") can interfere with attempts to relate $K_{d,\lambda}$ to other optical properties when these contribute a significant fraction of the detected irradiance (Haltrin et al., 1997; Gordon, 1999). Measurement of spectral reflectance ratios (either irradiance reflectance, E_u/E_d, or radiance reflectance, L_u/E_d) can suggest the wavelengths and depths where such interference is occurring (Haltrin et al., 1997) but must account for self shading of the upwelling signal when a large instrument package is deployed (Dierssen & Smith, 2000).

For depth-specific measurements the equation is

$$K_d = Log_e(E_{d,Z_1} / E_{d,Z_2}) / (Z_2 - Z_1) \quad (1)$$

where E_d is downwelling cosine irradiance measured at two depths, Z_1 and Z_2 (Kirk, 1994a; Kirk, 1994b). When E_d is measured continuously with depth by a UV profiling instrument the equation becomes

$$E_{d,Z_2} = E_{d,Z_1} e^{-K_d (Z_2 - Z_1)} \quad (2)$$

The value of K_d in equation (2) is typically estimated for a specific wavelength (λ) by regression analysis, solving for the slope of the straight line formed by plotting $Log_e(E_{d,Z})$ versus depth, Z, after correcting $E_{d,Z}$ for dark signal & other noise (Hargreaves, 2003). With either method an average value for $K_{d,\lambda}$ is attributed to a specific depth range. The value of $K_{d,\lambda}$ will be approximately constant throughout depths that are uniformly mixed but can increase or decrease somewhat with depth until an equilibrium extent of diffuseness develops (Gordon, 1989). Variations in K_d near the surface of well-mixed water are related to surface waves (Zaneveld et al., 2001) and to changes in diffuseness determined by sky conditions and sun angle (up to 20–25% for UV wavelengths, Hargreaves, 2003). It is because of the response of K_d to diffuseness and light angle that K_d has been called an apparent optical property (AOP) of the water body, in contrast to inherent optical properties discussed below.

K_d and other optical measurements respond to the concentration of particulate and dissolved matter and can be used to investigate factors controlling transparency of natural waters. In addition to K_d, (an AOP) these include inherent optical properties of the water, or IOPs (Tyler & Presiendorfer 1962), properties controlled by the composition of the water and not influenced by the light field. IOPs include the beam absorption coefficient, *a*, the beam scattering coefficient, *b*, and their sum, the beam attenuation coefficient, *c*. Direct measurement of *c* in the water column has been common for years using the beam transmissometer, typically with a red (e.g. 660 nm) light source. When measured at a long wavelength where CDOM absorption is negligible, variations in *c* are correlated with the concentration of particles because of their impact on scattering. Particulate organic carbon (POC), microbial biomass, or phytoplankton cells are the dominant particles in many aquatic systems (Boss et al., this issue). At the typical

wavelength of 660 nm used in transmissometers to measure beam *c*, the relatively constant absorption of water (c_{w660} = 0.411 m^{-1}, varying slightly with temperature, Pope & Fry 1997; Morel 1974; Pegau etal., 1997) can be subtracted to yield the particulate beam attenuation coefficient, c_{p660}.

Field measurements of *a* and *b* are relatively rare in visible wavelengths and extremely scarce in UV wavelengths (but see Boss et al., this issue). The value of *a* is the optical sum of absorption by dissolved and particulate constituents of natural waters in combination with a_w, absorption by H_20. The primary contributor to absorption by dissolved constituents in natural waters is colored dissolved organic matter (CDOM); a_{cdom} is typically measured using a laboratory spectrophotometer after particles are removed from the water sample by filtration. Values for a_{CDOM} can also be estimated from measurements of DOC concentration if DOC-specific absorption can be estimated as well. Although suspended mineral particles can sometimes make a large contribution to attenuation, especially in shallow water or near inflow from glaciers or rivers, the optically-important particles in lakes are typically phytoplankton. Spectral absorption by phytoplankton can be measured in a spectrophotometer by concentrating a water sample onto a glass fiber filter. While primarily used for visible wavelengths (Yentsch & Phinney, 1989; Mitchell 1990; Lohrenz 2000), the technique has also been used for UV wavelengths (Ayoub et al., 1996; Sosik, 1999; Helbling, et al., 1994; Belzile et al., 2002; Hargreaves 2003; Laurion et al., 2003).

Indirect measures of optical properties can be predictive of phytoplankton abundance and $K_{d,UV}$ in low-CDOM systems. The concentration of the primary photosynthetic pigment in phytoplankton (chlorophyll a) can be detected *in vivo* by its red absorption peak (676 nm) or by fluorescence measurements (emission peak at 683 nm) in the water column. Solar-stimulated

fluorescence from phytoplankton pigments can also be detected by spectral reflectance meters after correction for Raman scattering. In natural waters the c_{p660} signal described above primarily responds to particle concentration because of scattering at 660 nm but when the particles are predominantly biotic, c_{p660} is expected to covary also with absorption and also attenuation at other wavelengths. None of these indirect measures is likely to be useful alone in predicting UV attenuation over a range of depths because of photoacclimation: the deeper phytoplankton adjust to dim light by increasing the efficiency of light utilization, the concentration of chlorophyll per cell, and the absorption per unit of chlorophyll, and decreasing the proportion of UV-screening pigments (MacIntyre et al 2002). Summing F_{chl} and c_{p660}, with proper adjustment of their relative contribution, might provide a useful index of changing UV attenuation with depth when direct measures of UV attenuation are unavailable.

Another optical measurement that should be related to $K_{d,UV}$ in UV-transparent systems is Secchi depth (Z_{SD}). Measurement of Z_{SD} has been used for many years as a simple transparency index of water quality (Larson et al., 1996a). The depth at which a 20 cm white disk is barely visible under ideal conditions (flat surface, no reflections from the surface, and adequate solar radiation) depends on a combination of scattering that obscures the image of the underwater disc and absorption that diminishes the light reaching the disk from the surface. The inverse of Secchi depth ($1/Z_{SD}$, unit m^{-1}) has been shown to correlate with $[K_d + c]$ where K_d and c are measured for the appropriate range of wavelengths dependent on the combination of human vision and peak transmission wavelengths (Tyler,1968; Preisendorfer, 1986,) and depth-averaged from the surface to Z_{SD}. Human visibility of black objects underwater has been shown to vary inversely with beam attenuation in green wavebands (530 nm, Davies-Colley, 1988; Zaneveld & Pegau, 2003) but the blue waveband is likely to be more important in the case of very clear water such

as Crater Lake. Because phytoplankton contribute to both scattering and absorption in blue wavelengths and typically have UV-absorbing protective pigments in a high UVR environment, blue attenuation and $1/Z_{SD}$ should be correlated with UV attenuation when the latter is affected by phytoplankton. In other studies where phytoplankton and suspended mineral sediments control transparency, Secchi depth has been correlated with K_d measurements for the PAR waveband and with the concentration of suspended sediments (e.g. Jassby et al., 1999). In systems where the relative contributions to optical attenuation by phytoplankton and suspended mineral particles are variable, the relationships among c_{p660}, $1/Z_{SD}$, K_d, and phytoplankton concentration would be expected to vary somewhat, with K_d less responsive to increases in scattering than the other two measurements.

METHODS

Site characterization

Crater Lake is located in Crater Lake National Park in southwest Oregon, USA, at an elevation (lake surface) of 1883 m. Most of the measurements reported here were made at Station 13 (42.95^{o}N, 122.08^{o}W) near the deepest part of the lake (589 m, Larson et al., 1996a, 594 m, Bacon et al., 2002). Because of the steep caldera walls rising to an average elevation of 2100 m, the lake watershed area projected to a flat horizontal surface is relatively small, only 14.7 km^2 or 28% of the 53.2 km^2 surface area of the lake (Larson et al., 1996a).

Crater Lake data archives

The Long Term Limnological Monitoring Program database maintained by the Crater Lake National Park staff was the source for Secchi depth, photometer profiles, weather data, LI-COR radiometer profiles, chlorophyll-a data, and CTD profiles with beam transmissometer and fluorometer data (Larson et al., 1996a). The longest record is for Secchi depths; these data were

screened to meet specific criteria, and with the exception of the first record (the white dinner plate lowered by Diller in 1896, Diller 1897), all Z_{SD} data represent 20 cm disk data recorded during non-stormy weather with good visibility through the water surface.

Measuring and modeling solar radiation and spectral diffuse attenuation

Published measurements of Crater Lake $K_{d,380}$ from the 1960s were obtained from several sources (Smith and Tyler, 1967; Tyler & Smith, 1970; Smith et al., 1973). A LI-COR scanning radiometer (model LI-1800uw) was the primary instrument for the new measurements of UVR irradiance and attenuation reported here (performance reviewed in Kirk et al., 1994). The self-contained programmable scanning radiometer records downwelling cosine irradiance at 2 nm intervals from 300–800 nm with a bandwidth of 8 nm. LI-COR post-collection software provided immersion corrections to maintain accuracy both above and below the water surface. To create a depth-series of spectra the instrument was programmed to scan every two minutes and was then lowered on the sunny side of a small vessel near mid-day to specific depths and held for timed intervals. On many occasions an incident PAR signal was recorded on deck during the underwater scans in order to detect changing sky conditions. For each depth-series of spectra the data were evaluated at specific wavelengths to compute spectral K_d for each pair of depths (typically at 5 or 10 m vertical spacing). The data were carefully examined for anomalies (identified as outliers in both spectral and depth plots of $K_{d,\lambda}$) caused by surface waves or clouds; the occasional anomalies were either eliminated by interpolation between adjacent wavelengths or depths. The depth assigned to each K_d was the average for the upper and lower pair of E_d measurements. The LI-1800uw was factory calibrated on 26 May 1995, 18 July 2000, and 23 January 2002.

On 20 August 2001 two other UV radiometers (from Biospherical Instruments) were also used to record water depth and temperature and up to 20 fixed wavelengths of downwelling irradiance (E_d) and upwelling radiance (L_u) using filter-based diode sensors at a rate of 5 spectra per second. A PUV-2500 profiling UV radiometer recorded seven downwelling channels (305, 313, 320, 340, 380, 395 nm with nominal 8 nm bandwidth and PAR, 400–700 nm) plus upwelling radiance in the chlorophyll-a natural fluorescence waveband (center =683 nm). A PRR-800 profiling reflectance radiometer recorded 19 channel pairs of upwelling radiance and downwelling irradiance (340–710 nm) and PAR. The PRR-800 was lowered in its normal orientation to measure E_d and L_u and also lowered inverted to record upwelling irradiance E_u. The data from the Biospherical instruments were binned at 2 m depth intervals using Log_e averages. To detect internal radiation sources that could interfere with interpretation of diffuse attenuation measurements we measured spectral reflectance ratios for a range of depths using the PRR-800 radiometer. To reduce near-surface noise cause by waves and ripples we used both running averages of K_d (combining several adjacent depths) and polynomial regression of Ln(Ed) versus depth from which K_d was then calculated.

On this date we also computed incident irradiance using a radiative transfer model (RTBASIC, Biospherical Instruments, Inc.; see Madronich, 1993 and Biospherical Instruments, 1998, for more details) for comparison with the LI-1800uw incident spectra. The parameters for the 8-stream disort model were set to account for noon PDT conditions near the time that optical profiles were collected: current solar zenith angle (34.4^o), barometric pressure (774 mbar based on elevation above sea level), nominal albedo (5%) and current column ozone (313 DU, URL: http://toms.gsfc.nasa.gov/). To compute a spectrum with a bandwidth comparable to the LI-1800uw (8 nm) and comparable reporting interval (2 nm), model values with 1 nm bandwidth

were first generated at 2 nm intervals from 296–804 nm. These initial model values were then converted to represent an 8 nm bandwidth by calculating geometric means spanning 8 nm around each 2 nm interval.

To calculate PAR (400–700 nm) from LI-1800uw data, values reported as W nm^{-1} m^{-2} were summed and then multiplied by 2 nm per record to get the energy in the band, W m^{-2}. Quantum PAR irradiance (μMol m^{-2} s^{-1}) at the surface was calculated from W m^{-2} by multiplying by 4.60 (Kirk 1994b). To interpolate to an intermediate wavelength (e.g. 305 nm from 304 and 306 nm measurements) we used the geometric mean of measured irradiance. To reduce surface noise caused by waves and ripples the scans near the surface were repeated and averaged, or computed using the incident scan as the upper value after reducing it by 5% for nominal reflectance.

Other optical and bio-optical measurements

Bio-optical signals (most of which were described in Larson et al., 1996a) were recorded by a SeaTech transmissometer (25 cm 660 nm) and Wetlabs, Inc. WetStar chlorophyll-a fluorometer integrated with a SeaBird CTD profiler. Beam attenuation c_{660} was calculated from 2 m binned transmittance data (c_{660}= -Ln(T)*100/25), then converted to c_{p660} by subtracting c_{w660}, the beam attenuation coefficient for pure water (0.411 from $c_w = a_w + b_w$; a_w from Pope & Fry 1997; b_w from Morel 1974). Previous estimates of c_{w660} (Smith & Baker, 1981; Zaneveld & Bartz 1984; Bishop 1986) used to calculate c_{p660} have been superseded by much-improved measurements of a_w (Pope & Fry 1997).

Particles and whole water were analyzed on several occasions for organic carbon content. On two dates in 1999 (corresponding to c_{p660} profiles) samples were collected from three depths in 30 L. Niskin samplers (acid-washed), transferred to 20 L acid-washed carboys and 4–8 liters

were filtered through pre-combusted GF/F filters. Filters were analyzed on a Carlo Erba NA1500 Carbon/Nitrogen/Sulfur Analyzer using GF/F filter blanks and cystine standards. Whole water samples were also collected similarly (Urbach et al., 2001) on three dates from 12 depths and analyzed for total organic carbon (high temperature combustion using Shimadzu TOC-5000). On two dates the measurements of particulate organic carbon (POC g C/m^3) at three depths were correlated with c_{p660} (binned at 2 m intervals) yielding an average relationship where c_{p660}=0.019*[POC uM C] (r^2=0.53). Because of the small number of samples and low r^2 value we used the relationship reported with greater precision by Boss et al. (this issue) where c_{p660}=0.032*[POC uM C]-0.024 (r^2=0.996) to calculate POC for all depths from c_{p660}. We adjusted the offset term each month for slight variations in transmissometer baseline in order to match the deep particulate signals to 0.38 μM C for depths 300–500m in all summer months.

On 20 August 2001 spectral absorption of particulate samples was analyzed. Water (500–1000 ml) from five depths was filtered on GF/F filters (Whatman, with nominal retention of diameters greater than about 0.7 μm). Optical density was measured with the filter attached to a quartz disk in a Shimadzu 1601UV spectrophotometer using a modified Quantitative Filter Technique (QFT, Yentch & Phinney 1989; Mitchell, 1990) adapted for UV wavelengths (Helbling, et al., 1994; Ayoub et al., 1996; Sosik, 1999) and corrected for pathlength amplification using the method of Lohrenz (2000).

Filter photometer depth profiles began with Utterback et al., (1942), using a custom-built underwater photometer in July 1940 (they employed Schott BG12 filters, URL http://www.us.schott.com/, and a Weston cell, described by Barnard, 1938; the combined response curve has a peak at 450 nm with half-maximum responses at 390 and 490 nm). During 1968–1991 several Kahl filter photometers with similar properties to the instrument described

above (Kahlisco, Inc. underwater and deck sensors equipped with clear, red, green, and blue filters over a photodetector cell, see Larson, 1972 for added details) were used to collect light profiles to a typical depth of 145 m. The blue filter data were converted to $K_{d,blue}$ by calculating transmittance ($E_{d,z}/E_{d,o}$) from raw deck (E_{do}) and underwater (E_{dz}) data and then converting this using $K_{d,blue} = Ln(E_{d,o}/E_{d,z})/(Z2-Z1)$. $K_{d,blue}$ was then averaged from 10 m to the Secchi depth (40 m if no Secchi depth). Irregular photometer $K_{d,blue}$ values near the surface were excluded as needed.

Proxies for $K_{d,UV}$

Least squares linear regressions were used to develop proxy $K_{d,UV}$ values from measured Z_{SD} (using $1/Z_{SD}$), $K_{d,blue}$, and $K_{d,380}$ averaged over the 0–40 m or the Secchi depth. To develop an empirical model for $K_{d,380}$ based on chlorophyl-a fluorescence and c_{p660} we used trial and error to adjust two parameters to minimize residuals in comparison with $K_{d,380}$ determined from LI-1800uw spectral scans. To compute $K_{d,320}$ and $K_{d,380}$ from $1/Z_{SD}$, $K_{d,blue}$ was computed as an intermediate step. When historical data were measured over a different range of depths than 0–40 m we used recent patterns of K_d versus depth to calculate adjusted values.

RESULTS

Spectral measurements of incident and underwater solar radiation

In the extremely clear water of Crater Lake the wavelengths penetrating most deeply were in the blue waveband (400–500 nm). Incident and underwater spectra recorded on 20 August 2001 (a date when the surface waters were unusually transparent) are shown on a logarithmic irradiance scale for a range of depths in Figure 1A. Incident irradiance measurements made with the LI-COR LI-1800uw scanning radiometer were validated by comparing with model data for incident irradiance under ambient conditions (also plotted); in most of the UV

range (310–400 nm) the ratio of Measured**:**Modeled ranged from 87% to 108% and averaged 96%. Underwater the solar radiation diminished with increasing depth; both short and long wavelengths were attenuated more rapidly than those in the blue range (400–500 nm), resulting in a broad peak from 400–500 nm at 80 m and a narrower peak from 460–480 nm at 160 m. The limit of detection of the LI-COR LI-1800-uw scanning radiometer (Kirk et al., 1994) is reached between 10^{-4} and 10^{-5} Watts m^{-2} mn^{-1}depending on the wavelength. For comparison with relative attenuation depths reported for other natural waters Figure 1B shows curves for both 10% and 1% attenuation depths across the UV and part of the visible spectrum derived from the data plotted in figure 1A. Figure 1A shows that underwater irradiance is attenuated fairly evenly by wavelengths from 390–490 nm (also evident in the low slope of Figure 1B for wavelengths >390 nm). The most rapid attenuation with depth was at wavelengths longer than 600 nm.

Spectral upwelling irradiance, E_u (Figure 2A, measured on the same date as Figure 1 data with a PRR-800 radiometer equipped with 18 filter wavebands (lowered in inverted orientation so that cosine irradiance sensors faced downward) suggests the quality of light that would be visible from above the surface. The peak waveband is 412 nm (violet), with a nearly constant intensity from 380–490 nm (UV-A through blue). Another peak at 683 nm (the red peak emission wavelength for chlorophyll-a fluorescence) is evident at all depths but more distinct below 30 m. Figure 2B shows the reflectance ratio of upwelling radiance (L_u) to downwelling irradiance (E_d) at different depths (PRR-800 was used in its normal orientation), with a regular spectral pattern of declining L_u:E_d at increasing wavelengths observed for shallow depths, but with increasing depth there is a dramatic rise in reflectance for longer wavelengths (>590 nm at 15 m depth, >565 nm at 25 m, and > 490 nm at 120 m).

Spectral diffuse attenuation, Validation, and Variations over Space and Time

Spectral diffuse attenuation ($K_{d,\lambda}$) is shown in Figure 3 calculated from the spectral irradiance data shown in Figure 1 (K_d was averaged from multiple scans for specific depth ranges and the standard errors of the mean for these are indicated by error bars). One additional depth range (10–18 m) not appearing in Fig 1A was calculated from Biospherical Instruments, Inc. (BSI) PRR-800 and PUV-2500 profiling radiometers. In the UV and blue wavebands K_d spectra were lowest near the surface and rose with increasing depth down to the deep chlorophyll maximum (DCM=130 m). The K_d pattern at wavelengths longer than 550 nm varied little with depth when measured near the surface but at depths deeper than 20–30 m and shallower at the longest visible wavelengths the K_d values declined with increasing depth (not plotted). LI-COR K_d spectra for shallow depths (not plotted) were similar to the plotted K_d spectrum from the BSI radiometers but were noisier because fewer measurements were used in the calculations.

Variations of K_d with depth for specific wavelengths on 20 August 2001 appear in Figure 4. The LI-COR UV wavelengths were selected to match the filter wavebands (320, 340, 380 nm and PAR) of two BSI radiometers (all three were deployed within about 1 hour of solar noon). The curves show a region of uniform and low $K_{d,UV}$ from 0–10 m (the thermally mixed layer was also 0–10 m), then a pattern of increasing $K_{d,UV}$ with depth to a peak at the DCM near 130 m. For broadband visible irradiance (PAR, 400–700 nm) the $K_{d,PAR}$ rose rapidly above 15 m but paralleled the other sensors at depths below 60 m. The three instruments agreed closely for most depths over which the same wavelengths were measured, with the greatest variation occurring near the surface. Figure 5 shows the same type of pattern but in this case averaged for the period 1996–2002. There are parallel changes with depth in $K_{d,320}$, $K_{d,380}$, and $K_{d,blue}$ (summarized also in Table 1). Figure 6 shows that the ratio of K_{d320}:K_{d380} varied regularly with depth (K_{d320}:K_{d380} = -0.0031*depth + 2.32, r^2=0.68) for the 1996–2002 summer data. In contrast, the ratios

$K_{d,320}$:$K_{d,blue}$ and $K_{d,380}$:$K_{d,blue}$ were relatively constant for two depth ranges: 0–10 m and below 10 m. Related optical changes with depth based on particle absorption coefficients are shown in Figure 12B (described below).

Seasonal and interannual changes in UV K_d near for different depth ranges are summarized in Figure 7. July and August were typically the months with the lowest $K_{d,320}$ averaged over 0–40 m, the depth range where maximal UVR impact on organisms was expected. If the single measurement in January is typical then winter values are much higher than mid-summer values for this depth range (Figure 7A). Over the period from 1996–2002 the lowest summer average $K_{d,320}$ was observed in 2001; the highest were in 1998 and 1999. When July and August data are averaged over this period the greatest interannual variations in $K_{d,380}$ occurred in the depths from 20–40 m and the least variations occurred from 100–140 m. The range from 0–20 m changed in parallel with 20–40 m except for 1999 (Figure 7B).

Proxy measurements for UV attenuation versus depth; Phytoplankton control of $K_{d,UV}$

Bio-optical signals provide several proxies for UV attenuation through the water column. The red beam transmissometer signal (from which c_{p660} is calculated) has been measured since 1987 in Crater Lake (Larson et al., 1996a) and provides an optical proxy particulate organic carbon (POC) and in the upper 80 m it can serve as a proxy measurement for UV attenuation. The rationale for using cp660 as a proxy for $_{Kd,UV}$ is described earlier. Depth profiles measured during 1999 for POC (calculated from c_{p660} based upon POC analysis of discrete samples), total organic carbon (TOC), and dissolved organic carbon (DOC, calculated as TOC-POC) are shown in Figures 8A–C. The POC signal in the upper 130 m was much higher than at deeper depths and in this shallower range it increased slightly from July to September. TOC values showed similar trends but were more variable, especially the few measurements at deeper depths (not plotted

below 150 m). The DOC values were of low accuracy because of combined errors in the POC and TOC measurements and difficulty of making low level measurements, but they show a similar seasonal trend to that for POC and TOC and a consistent small peak near a depth of 80 m.

On some occasions when there has been an influx of suspended inorganic particles the c_{p660} signal does reflect the concentration of POC. Figure 9A shows a series of c_{p660} depth profiles during 1995, a summer that experienced a late snowmelt, and several large rain storms in June and July. Extra peaks are apparent in Figure 9A above 25 m and below 200 m. The change in this turbidity signal over time is plotted in Figure 9B for both the near-surface water (0–20 m) and representative deep water (>300 m) along with comparison data for the typical (dry) summer of 1994, when the deep cp660 remained low throughout the summer.

Chlorophyll-a concentration can also serve as a proxy for UVR attenuation. Figure 10A shows the average concentrations from 1984–2002 for shallow (0–30 m) and deep (40–140 m) chlorophyll-a extracted from phytoplankton retained on a 0.45 micron filter. Also plotted is average monthly rain in July and August for this period. Except for 1986–1987 the deep and shallow concentrations tended to change roughly in parallel, with a maximum during the late 1980s and low values since 1996. Figure 10B shows the variations in $K_{d,320}$ (estimated by our Secchi depth proxy) plotted against the chlorophyll-a concentration in the 0–30 m depth range. The regression line for the dry months or months where precipitation occurred as snow or where runoff would have entered cold surface waters ($y = 015x + 0.08$, $r^2=0.44$) indicates that during periods with little runoff retained in the upper mixed layer about 44% of the variation in UV attenuation is explained by the absorption and scattering in UV wavelengths that co-varies with chlorophyll-a concentration.

Another bio-optical signal, chlorophyll-a fluorescence (F_{chl}), has been recorded in Crater Lake depth profiles since 1999 and provides a proxy for UV attenuation consistent with the dominant role of phytoplankton absorption and scattering. Figure 11A shows $K_{d,380}$ and F_{chl} for 20 August 2001 and the correspondence between the two signals is apparent. However at depths above about 80 m there are subtle differences between the two signals and for this upper part of the photic zone $K_{d,380}$ more closely resembles the cp660 signal (also plotted in Figure 11A). A simple empirical model estimates $K_{d,380}$ (heavy curve in Figure 11A) from c_{p660} and F_{chl} (μg/L from fluorescence) by combining the two bio-optical signals: $K_{d,380}=0.40*F_{Chl}+0.36*c_{p660}$. The F_{chl} and c_{p660} signals are also combined in a ratio (F_{chl}/c_{p660}) in Figure 11B to show changes with depth and season for 2001 as a proxy for chlorophyll-a:carbon ratios. Figure 11B shows a distinct peak near the surface on 14 August (20–40 m) and a smaller surface peak on 20 August (40–60 m). Ratios on all dates increased with depth to a maximum corresponding to the DCM. Below the DCM the pattern varied with season, generally declining during the course of the summer.

Possible UVR Impacts on the Crater Lake Ecosystem

Optical absorption by phytoplankton contributes directly to diffuse attenuation and absorption spectra can also reveal a protective response of phytoplankton to UVR exposure. Figure 12A shows spectral absorption measurements for five depths made 20 August 2001 on GF/F glass fiber filters. Distinct chlorophyll-a peaks are visible at 430 and 675 nm. Chlorophyll-a concentrations calculated from 675 nm peaks (0.038–0.38 mg m^{-3} using $ap^*_{675}=0.040$) closely match the [Chl-a] calculated from data in Fig 3 using the diffuse attenuation model of Morel and Maritorena 2001. Typical $ap^*_{675} = 0.035$ according to Sathyendranath et al. (1987).

The arrow in Figure 12A indicates a peak at 325 nm that appears clearly at depths of 25 and 50 m. This wavelength is consistent with UV-B protective compounds called micosporine-like amino acids or MAAs (Tartarotti et al., 2001) known to be produced by certain phytoplankton when exposed to UV-B radiation. Figure 12B shows depth trends for UV-B irradiance ($E_{d,\,320}$), particulate absorption ratios (a_{p330}:a_{p675} and a_{p440}:a_{p675}), and the F_{chl}:c_{p660} ratio (from the 20 August 2001 curve in Figure 11B). The ratio a_{p330}:a_{p675} follows a similar declining trend with depth as observed in $K_{d,320}$:$K_{d,380}$ ratios (Figure 6), suggesting that phytoplankton produce more MAAs relative to photosynthetic pigments when exposed to strong sunlight containing UV-B.

One possible response to strong UVR in an aquatic ecosystem is inhibition of growth and survival for members of the plankton community. The low concentration of chlorophyll observed near the surface (Figures 10A, 11, 12A) and scarcity of other organisms (Larson et al., 1996b) are consistent with this impact but other factors such as nutrient limitation could also be a dominant factor. A natural experiment with solar UV-B radiation has taken place over the past 20 years because of daily, seasonal, and interannual variations in stratospheric ozone above Crater Lake. Figure 13A shows the record of stratospheric ozone (averaged for several weeks before the typical mid-month sampling dates for phytoplankton). Also plotted are the chlorophyll-a concentrations from Figure 10A. The large variations in phytoplankton apparent in Figure 13A may be partly explained by atmospheric variations in ozone that lead to inverse variations in UV-B radiation reaching the lake surface. Figure 13B shows the positive regression relationship between chlorophyll-a and stratospheric ozone (Chl-a, 40–140 m: $y = 0.025x - 7.4$, $r^2 = 0.49$; Chl-a, 0–40 m: $y = 0.004x - 1.07$, $r^2 = 0.27$) consistent with UV-B irradiance

accounting for 27–49% of the variation in phytoplankton pigment concentration either directly, or by inhibiting predators that feed on phytoplankton grazers.

Long-term Proxies for $K_{d,UV}$ and Decadal Changes in UV Transparency

Several proxies for UV attenuation can be used to look at long term changes in UV transparency because of the long time period covered by the primary measurements. The signal most similar to $K_{d,UV}$ is $K_{d,blue}$ measured by photometers equipped with changeable filters on deck and underwater sensors. LI-COR LI-1800uw radiometer data averaged over depths 0–40 m and for the period 1996–2002 were used to calculate K_d plotted in Figure 14A. These were used to derive regression equations (see Figure 14A caption) relating $K_{d,blue}$ (nominally 400–500 nm) to $K_{d,320}$ and $K_{d,380}$ (1996–2002). We then applied the equations to historic $K_{d,blue}$ data (gathered by photometers equipped with blue filters in 1940, 1969 and 1980–1991) to estimate $K_{d,320}$ and $K_{d,380}$. Figure 14B shows the time series for $K_{d,320}$ and $K_{d,380}$ derived from direct UV measurements (black symbols), from $K_{d,blue}$ measurements with blue-filter photometers (light gray squares and triangles), and from radiometer measurements of only $K_{d,380}$ values (dark gray triangles) where $K_{d,320}$ was calculated using the relationship in Figure 6. Based on this collection of direct and indirect calculations the lowest $K_{d,320}$ (0.066 m^{-1} estimated from radiometer-measured $K_{d,380}$) occurred in 1966; $K_{d,320}$ in 2001 was nearly identical (0.068 m^{-1}). The range among the annual summer averages for $K_{d,320}$ during this period (0.07 to 0.12 m^{-1}) represents approximately 35% variation above or below the mean.

The longest optical record in Crater Lake is from measurements of Secchi depth, beginning in 1896 (Larson et al., 1996a). The inverse of Secchi depth ($1/Z_{SD}$) should be correlated with other apparent and inherent optical properties as described earlier. When $K_{d,blue}$ is calculated from blue-filter photometer data and averaged from the surface to the Secchi depth

measured on the same day, 13 years of summer averages (June–August) are well-correlated with $1/Z_{SD}$ (Figure 15A, $K_{d,blue} = 2.08/Z_{SD} - 0.026$; r^2=0.54, N=13). Figure 15B compares $K_{d,blue}$ calculated from $1/Z_{SD}$ for the period 1937 through 2002 with $K_{d,blue}$ measured by photometer (averaged to Z_{SD} or 40 m) and by radiometer (averaged to 40 m). The agreement among $K_{d,blue}$ summer averages (July–August) from Photometer and $1/Z_{SD}$ data (regardless of whether data were collected on the same day) was within +20% and -28% for the 12 years where both two types of data were available. Comparing $K_{d,blue}$ derived from radiometer and Z_{SD} the agreement was within +7% and -35%. The largest difference between radiometer and $1/Z_{SD}$ averages occurred in 2000 when the summer averages were 0.046 m^{-1} from all $1/Z_{SD}$ data and 0.031 m^{-1} from the two radiometer dates (June and August). The agreement improved when only $1/Z_{SD}$ data collected within 2 days of the radiometer profiles were compared (agreement of summer averages was then within 1.5%). Differences can also be expected in part because instrument profiles covered 0–40 m while Secchi depth summer averages ranged from 23–38 m during the period 1896–2002.

Using the relationships described above for estimating $K_{d,blue}$ from Secchi depth measurements and for estimating $K_{d,320}$ and $K_{d,380}$ from $K_{d,blue}$, we calculated $K_{d,320}$ and $K_{d,380}$ for the period 1896–2002. The resulting record of UV attenuation (averaged from the surface to depths ranging from 23–44 m, depending on the Secchi depth) is shown in Figure 16A from 1937–2002 along with radiometer-derived and photometer-derived values. In years when LI-1800uw radiometer or photometer records coincide with Secchi depth data there is a general correspondence between estimates except for a few years (early 1980s and 2000). The large spike in 1995 is based only on Z_{SD} measurements although c_{p660} data confirm the high attenuation near the surface (Figures 9A & 9B). The range for $K_{d,320}$ based on Secchi depths is

0.08–0.19 m^{-1} (maximum 0.15 excluding 1995); based on the blue photometer data it is 0.08–0.15 m^{-1} (no measurements in 1995); based on the LI-1800uw it is 0.07–0.10 m^{-1} (1996–2002). From the detailed measurements starting in the 1978 there is a decadal pattern of peaks and valleys with amplitude of roughly +/- 50%, scattered with infrequent spikes of higher attenuation (e.g. 1995). By averaging all sources of data for $K_{d,320}$ for each year (Figure 16B) the range and pattern from 1896–1969 was plotted. The values ranged from 0.07–0.14 m^{-1} from 1978–2002, and from 0.07–0.12 m^{-1} from 1896–1969.

DISCUSSION

Spectral measurements of incident and underwater solar radiation

Spectral measurements of downwelling irradiance (Figure 1A), upwelling irradiance (Figure 2A), spectral K_d (Figure 3) in August 2001 were nearly identical to the 1960s data of Smith et al 1973 except that the recent measurements included a greater range of wavelengths, responded to lower light levels, and in the case of E_u, resolved algal fluorescence distinctly at 683 nm. The LI-1800uw has been shown previously to record solar irradiance accurately within the constraints of its 8 nm bandwidth except at wavelengths below 308 nm (Kirk et al., 1994). Figure 1 demonstrates similar performance: matching within 96% on average and -13% and +9% at all wavelengths from 308 to 400 nm in comparing a scan of incident irradiance with a spectrum generated by a high resolution radiative transfer model adjusted for local conditions and bandwidth.

Figures 2A and 2B show signs of "internal light sources" including chlorophyll-a fluorescence (683 nm), Raman scattering (impact at shorter wavelengths from 700–490 as depth increases), and possibly phycoerythrin fluorescence (589 nm, Hewes et al., 1998). The fluorescence signals indicate the presence of phytoplankton but cannot be directly used as

indices of concentration because of photoacclimation and quenching near the surface. The detection of any internal source should serve as a warning because it invalidates attempts to measure diffuse attenuation at the wavelength and depth where it is detected.

While the conventional method of characterizing potential exposure to UVR is to measure diffuse attenuation, another factor which strongly influences exposure is incident irradiance. Our discovery of a positive correlation between phytoplankton chlorophyll-a and stratospheric ozone means that variations in incident UV-B irradiance could be playing an important role and thus UV-B irradiance should be monitored continuously on or near the lake.

The upwelling irradiance (Figure 2A) and radiance spectra (not shown) help to explain the unusual color of Crater Lake. The low concentration of absorbing substances (e.g. phytoplankton and CDOM) near the surface clearly accounts for part of the phenomenon, thereby allowing for a greater optical role for water molecules to transmit and scatter light of certain wavelengths. Spectral reflectance models that predict the optical behavior of pure water (e.g. Morel & Prieur 1977) indicate that while Crater Lake has extremely low levels of absorbing substances near the surface, it also contains particles that increase backscatter (for more on scattering, see Boss et al., this issue). The optical role of abundant glass-like suspended particles reported in the surface waters by Utterback et al. (1942) should be investigated.

Comparison of spectral measurements from 1969 in Crater Lake with similar measurements in Lake Tahoe (Smith et al., 1973) showed that Crater Lake had a greater proportion of short wavelengths in its upwelling spectrum and in the deep downwelling spectra. The differences between these two lakes appear to have increased since 1969 because of rising levels of nutrients, phytoplankton, and suspended mineral particles in L. Tahoe (Jassby et al., 1999).

Spectral diffuse attenuation, Validation, and Variations over Space and Time

In Crater Lake several intercomparisons have been carried out that have confirmed its ability to measure spectral diffuse attenuation accurately under extremely transparent conditions (e.g., Figure 4). The primary limitations of the LI-1800uw in Crater Lake are the inability to accurately record wavelengths shorter than 308 nm, and the time required to complete a scan when irradiance is changing rapidly (e.g. within 15 m of the surface). Measurements of diffuse attenuation would not benefit from higher spectral resolution than its 8 nm bandwidth, in contrast to measurements of solar irradiance spectra, except in the case of the shortest UV-B wavelengths. This is because spectra of typical attenuating substances tend to vary gradually with wavelength, and because there are instrument performance tradeoffs so that increasing spectral resolution leads to decreasing sensitivity to low light levels underwater (Kirk et al., 1994). While the effective center wavelength of a broad irradiance waveband can change as a function of depth (Hargreaves, 2003), the LI-1800uw has been tested previously in lakes with substantially more CDOM than Crater Lake and proved capable of generating accurate K_d values there in comparison with BSI radiometers and a scanning radiometer that had a 2 nm bandwidth (Kirk et al., 1994).

The surface waters of Crater Lake are remarkably transparent to UV-B radiation. The relative attenuation of solar UV-B (320 nm) at a depth of 20 m in Crater Lake was 27% of surface irradiance on average (Table 1). Both the average $K_{d,320}$ of 0.062 m^{-1} (1996–2002) and minimum $K_{d,320}$ (August 2001, 10–18 m average) of 0.057 m^{-1}, for the surface of Crater Lake were more transparent to solar UV-B than attenuation estimated for pure water ($K_{dw,320}$ = 0.09 m^{-1}, Smith & Baker, 1981). On only a few other occasions have such low values $K_{d,UV-B}$ been reported for natural waters. An ice covered lake in the dry valleys region of Antarctica (L.

Vanda) had low levels of phytoplankton and DOC and $K_{d,320}$=0.055 m^{-1} near its surface (Vincent et al., 1998). An earlier study (Goldman et al., 1967) reported that the upper water column in L. Vanda was remarkably clear and similar to pure water based on blue photometer measurements ($K_{d,blue}$=0.031 on one occasion, identical to $K_{d,blue}$ average over 0–40 m for Crater Lake in July 1940, Utterback et al., 1942). In a region of the Gulf of Mexico away from the influence of Mississippi River runoff (flowing at the lowest rate in 52 years during July 1988 when measurements were made) Højerslev and Aarup (2002) reported $K_{d,310}$=0.071 m^{-1}. This value is equivalent to $K_{d,320}$=0.061 m^{-1} after wavelength conversion (using the exponential equation for CDOM absorption of Bricaud et al., 1981, but without the backscatter correction suggested by Markager & Vincent, 2000, using an exponent of -0.015 derived from regressing Crater Lake spectral K_d, averaged 0–40 m on 20 August 2001, against wavelengths from 305–380 nm). Morel and Maritorena (2001) also reported extremely low values ($K_{d,305}$=0.095, or $K_{d,320}$=0.076, converted as described above) for oligotrophic regions of the tropical Pacific Ocean where chlorophyll-a varied from 0.043–0.054 mg m^{-3}over depths 0–72 m. In each of these published reports of extremely low UV-B attenuation the authors noted the discrepancy between their measurements and the Smith and Baker (1981) estimates for K_w for pure water. Hargreaves (2003) estimated the UV-B attenuation of pure water from Crater Lake measurements; the new estimate ($K_{dw,320}$=0.045) represented a 50% reduction from the 1981 estimate. Other cases of extreme transparency probably exist where water is isolated from organic soils and algal productivity or other sources of CDOM by temperature, altitude, water currents, and strong solar UVR and where photobleaching can reduce absorption by any CDOM that is present.

From Figures 4 and 5 one can see that the surface of Crater Lake typically has the greatest transparency but measurements here are problematic because of optical noise caused by

waves and ripples reflecting and redirecting sunlight (Zaneveld et al., 2001). While a comparison of irradiance ($E_{d,0+}$) just above the surface with $E_{d,Z}$ at a depth of 15 or 20 m should remove much of the noise attributed to surface waves, this approach introduces uncertainty about the wavelength-specific transmittance through the air-water interface. With a profiling radiometer it is easier to compensate for this noise by lowering the instrument slowly in the upper 15 meters so that multiple readings are available for averaging (of log-transformed irradiance) within 1 m, 2 m, or larger "depth bins". Another method (we used this to generate the 10–18 m curve in Figure 3) involves fitting polynomial regressions to $E_{d,Z}$ versus Z for each wavelength of interest, taking care to use a sufficient number of significant figures for fitted parameters and to avoid extrapolation beyond the bounds of the fitted data. From the regression equations for each wavelength the specific values of $E_{d,Z}$ can then be calculated at several depths close to the surface and from these $K_{d,Z}$ can be calculated.

Morel and Prieur (1977) have used Crater Lake as an example of Case 1 natural water in their ocean classification scheme on the basis of autochthonous control of transparency. One indication of the oceanic nature of Crater Lake is the convergence of K_d spectra in Figure 3 and model K_d (not shown) calculated from the bio-optical model of Morel and Maritorena (2001). After increasing their values for K_{water} slightly (4.5%) to match the measured K_d at longer wavelengths not affected by phytoplankton, it was possible to fit each curve in Figure 3 with a calculated K_d spectrum from 350–550 nm by adjusting a hypothetical chlorophyll-a value from which the model calculates K_d. On 20 August 2001 these fitted values for different depths ranged from 0.03–0.33 mg m^{-3} chlorophyll-a and compared well with chlorophyll-a concentrations estimated from particulate absorption at 675 nm (Figure 12A), which ranged from 0.04–0.38 mg m^{-3} using a specific absorption coefficient at 675 nm of 0.04 m^{-1} per mg m^{-3}. For chlorophyll-a

measurements from samples collected on 14 August 2001 and 11 September 2001 (chlorophyll-a extracted from 0.45 micron filters) the concentration of chlorophyll-a in the 0–30 m range of depths was 0.014 mg m^{-3} and the value near the DCM was 0.12 mg m^{-3}.

Seasonal and interannual variations in radiometer-derived $K_{d,320}$ and $K_{d,380}$ (Figures 7A and 7B) were small but significant during the period 1996–2002 but few UV measurements are available from earlier years. The first Crater Lake UV measurement (August 1964) used an experimental instrument to characterize spectral horizontal radiance reflectance, 400–700 nm (Tyler 1965). Although the spectrum was clearly related (inversely) to absorption in the upper meter of the water column, it is difficult to compare because of the unconventional approach. Measurements in August 1966 of upwelling and downwelling spectral irradiance to 25 m from 360–700 nm were more useful (Smith & Tyler, 1967; Tyler & Smith, 1970). When we recomputed K_d from reported E_d values at 0, 5, 15, and 25 m we discovered substantial noise in the blue and UV wavelengths but used an exponential model (Bricaud et al., 1981) to estimate K_d at 380 nm from wavelengths 360–390 nm (depth-averaged K_d using 5–15 and 15–25 m E_d data pairs) and then adjusted for shallow depths using the relationship in Figure 5 to compare with K_d averaged over 0–40 m (Figure 12). After these adjustments the values were still historically at the low end of observed K_d suggesting that Crater Lake was extremely clear during the 1960s. The data collected in August 1969 included upwelling and downwelling spectral irradiance to 99 m over 360–700 nm (Smith et al., 1973) but no tables were provided; values were estimated from published graphs and showed that Crater Lake was similar in transparency to the average of the recent period (1996–2002). For both 1966 and 1969 the values for $K_{d,320}$ were not measured but were estimated from measured $K_{d,380}$ using the average relationship in Figure 6.

Larson et al. (1996a) discussed determinants of visual clarity in Crater Lake, primarily phytoplankton and abiotic particles (storm-related suspended mineral sediments). Only a few other cases of phytoplankton influencing UV attenuation in clear lakes have been reported (e.g. Sommaruga 2001). While we have argued above that phytoplankton control attenuation during dry periods (see Figures 10B, 11A, 12A), there probably exists a contribution to K_d from suspended allochthonous particles (mineral particles and pollen) at all times (Morel & Prieur, 1977). This contribution may vary in response to wind, turbulence, and proximity to shore. Even without the uncertain contribution of suspended minerals, chlorophyll-a is not a perfect predictor of UV attenuation if phytoplankton vary in their composition of accessory pigments and MAAs. The additional contribution of CDOM produced by phytoplankton requires more investigation given the observation of Boss et al. (this issue) that CDOM increases with depth and during the summer. The possible impact of fires on UV transparency has not been addressed but fires could influence $K_{d,UV}$ directly (smoke particles entering the water) and indirectly (e.g. influencing turbidity and nutrients in runoff).

Proxy Measurements for UV Attenuation Versus Depth

A number of indirect proxy measurements for UV attenuation have been utilized in our study. Proxies can be useful when conditions are not appropriate for measuring $E_{d,Z}$ directly (e.g. rapidly changing sky conditions, or low sun angle) or when a UV radiometer is not available. Many take advantage of some optical property of phytoplankton (e.g. scattering of the red beam of a transmissometer (e.g. 660 nm), fluorescence (F_{chl}, 683 nm), absorption at the red chlorophyll-a peak (675 nm) or over the blue part of the visible spectrum (400–500 nm). The strong correlation of F_{chl} from chlorophyll-a and $K_{d,380}$ (Figure 11A) can be caused by the direct absorption of UVR by chlorophyll-a, but is also likely to vary with depth and UV wavelength

because of the absorption of other molecules such as MAAs and because photoacclimation and photochemical quenching change the relationship between F_{chl} and [chlorophyll-a] (Boss et al., this issue). Variation in accessory and UV-B screening pigments is suggested by the changing ratios of K_{d320}:K_{d380} in Figure 6, and of a_{p330}:a_{p675} in Figure 12B. It is not uncommon in clear aquatic systems for the biomass peak to occur at a different depth from the chlorophyll-a maximum (Fennel & Boss, 2003).

The concentration of dissolved organic carbon (DOC) has frequently been used as a proxy for UV attenuation (reviewed in Hargreaves, 2003) but measurements in Crater Lake are limited to a few dates and low reproducibility (Figure 8). Measurements of phytoplankton absorbance can be complicated by the tendency for MAAs to be released from phytoplankton during filtration (Laurion et al., 2003) as this will tend to cause elevated values in CDOM measured after filtration, and by the limits of detection using a 10 cm cuvette and laboratory spectrophotometer (but see Boss et al., this issue, for a long-pathlength *in situ* method). Published equations relating $K_{d,320}$ and DOC concentration (Hargreaves, 2003) vary because of the optical quality of DOC (photobleaching and source contribute to this variation). At low [DOC] the fit of this type of equation also is likely to depend on a correlation of [DOC] with [phytoplankton] because of the low absolute absorption by CDOM relative to phytoplankton. Within the uncertainty of the DOC measurements, Crater Lake is similar to the extremely transparent Lake Vanda, Antarctica. Comparing the DOC and UV attenuation data for L. Vanda and Crater Lake, Vincent et al., (1998) reported L. Vanda DOC = 0.3 g/m^3 and $K_{d,320}$=0.055, while our data for Crater Lake during summer 1999 (averaged over 0–40 m), show DOC = 0.1 g m^{-3} and $K_{d,320}$ = 0.09 m^{-1}. At this low level of DOC concentration the technique to account for instrument blanks is crucial (Sharp et al., 1993). The large difference in DOC-specific UV-B

attenuation ($K_{d,320}$-$K_{dw,320}$):DOC = 0.03 for Lake Vanda and 0.5 for Crater Lake 0–40 m in 1999) suggests either a difference in DOC measurement technique or a difference in the optical contributions of phytoplankton and a_{CDOM}, for example by photobleaching of a_{CDOM} in Crater Lake.

To our knowledge particulate organic carbon (POC) has not been used as a proxy for $K_{d,UV}$. In Crater Lake we observed that UV attenuation can be characterized by a combination of c_{p660} and F_{chl}, the former more important near the surface and the latter more important at greater depths (Figure 11A). This relationship seems reasonable in an oligotrophic lake with low levels of DOC because the c_{p660} detects scattering by cells when absorption by chlorophyll-a is suppressed at high light levels in the process of photoacclimation. The cells at shallower depths will still be attenuating UV wavelengths because of their inevitable content of other UV-absorbing molecules. Figure 11B clearly shows the consequence of photoacclimation in the phytoplankton community as the chlorophyll-a concentration per unit of carbon (and presumably per cell) is reduced at depths shallower than 50–75 m. Below this range of depths the chlorophyll-a concentration and the effective light absorbing properties of chlorophyll-a are increased as phytoplankton adapt to low light conditions. Along with the chlorophyll-a there are accessory pigments and macromolecules that absorb UVR. It is not clear how the pattern in Figure 11B is modified by exposure to the high levels of UVR because one can imagine something similar would result simply from exposure to visible wavelengths. And where ever the microbial community develops in the water column, one can expect to find detrital particles and dissolved DOC co-varying with the living cells.

While depth profiles of c_{p660} typically show the pattern for biomass distribution in Crater Lake suggesting a biomass peak ranging from 50–100 m (Boss et al., this issue) the c_{p660} signal

also detects scattering caused by suspended mineral particles entering with runoff from heavy rain. The seasonal and depth patterns of c_{p660} for 1995, a year with unusually high optical attenuation and heavy summer rain, demonstrate the slow transport of sediments from the surface to the bottom. Depth profiles for 1995 (Figure 9A) showed an unusual c_{p660} peak in turbidity close to the surface during July and August and peaks deeper in the water column (>250 m) that were not present in other years. A time course for the near-surface and near-bottom c_{p660} signal in Figure 9B compares 1994, a more typical dry year, with 1995. During June and July of 1995 the Crater Lake weather records included several precipitation events and an unusually late time (5 July) for melting of the snow pack at the Park Headquarters weather station and one of the authors (MWB) recorded observations of downslope sediment transport into the water and turbidity in the lake surface in response to these storms. Water column peaks in the c_{p660} signal could be caused by mineral particles or phytoplankton. Records of [chlorophyll-a] averaged over 0–30 m do not show elevated values for July 1995 compared to other years (Figure 15A). Turbidity traveling down the water column has appeared in transmissometer records from other years (e.g. 1991, 1996, 1997, 1998) but the entry of turbidity from runoff down the slopes and into the surface waters, followed by spreading across the lake by wind driven currents has only been reported for 1995.

Long-term Proxies for $K_{d,UV}$

Development of the $K_{d,blue}$ signal as a proxy for $K_{d,UV}$ can be justified from empirical observations in Crater Lake. The attenuation spectra (e.g. Figure 3) near the surface are relatively flat over the response waveband of the combined blue filter and Weston cell sensor using in underwater photometers (Crater Lake K_d averaged over 0–30 m varied spectrally by +36% ($K_{d,500}$) and -12% ($K_{d,400}$) compared to the mean $K_{d,400–500}$; the response bandwidth was 390–490

nm or nominally 400–500 nm). Also, the $K_{d,UV}$ values measured with the LI-1800uw radiometer gave nearly constant or predictable ratios for $K_{d,320}$:$K_{d,blue}$, $K_{d,380}$:$K_{d,blue}$, and $K_{d,320}$:$K_{d,380}$ in the upper water column (Figure 6). While the LI-1800uw radiometer has not been directly compared with a Kahl blue-filter photometer, the agreement is excellent (Figure 14B) between $K_{d,blue}$ from UV radiometer and photometer measurements in 1969 that occurred within 10 days of each other. $K_{d,UV}$ values from radiometer and photometer measurements made in the 1960s were similar to the data from 1996–2002 while on average the $K_{d,UV}$ values estimated by proxies from the 1980s were higher.

A combination of scattering and absorption contribute to Secchi depth signal and several theoretical and empirical papers have discussed the proportional relationship of $1/Z_{SD}$ and K_d+c_p (Tyler, 1968; Preisendorfer, 1986). Our proxy relationship between $1/Z_{SD}$ and $K_{d,blue}$ is based on same-day measurements starting in 1968. While one cannot assume that c_p and K_d will change in parallel as conditions in the lake change, we have used the empirical pattern to establish an equation ($K_{d,blue} = 2.08/Z_{SD} - 0.026$; r^2=0.54, N=13 years) and then convert $K_{d,blue}$ to $K_{d,320}$ or $K_{d,380}$ using the relationship described above. Although there are many possible sources of error in the proxy approach relating $K_{d,UV}$ and $1/Z_{SD}$, we estimate from regression residuals (Figure 15A) that annual averages of $K_{d,320}$ estimated from $K_{d,blue}$ will fall within 12% of the values measured with a radiometer. This calculation assumes that conditions from 0–40 m remain within the bounds that Crater Lake has experienced between the earliest paired measurements in 1968 and the present.

Decadal Changes in UV Transparency

Comparisons of our UVR attenuation measurements with those from radiometer data in the 1960s and from frequent proxy measurements since 1978 suggest that UV attenuation

changes on decadal and longer cycles, perhaps in response to a combination of rain and stratospheric ozone influencing the phytoplankton community, with heavy summer rain occasionally influencing the level of suspended mineral particles. We also cannot rule out the impact of trophic interactions and winter precipitation or nutrient upwelling as additional factors influencing phytoplankton. Given the modest level of variation that our phytoplankton model accounts for, it is also possible that substantial variations in attenuation are caused by wind-driven changes in suspended mineral particles during dry periods. One possible explanation for lower average blue attenuation since 1992 (excluding storm-related peak in 1995) is the improvement to sewage disposal at the tourist facilities in 1991 (Larson 2002). This hypothesis is considered unsupported by phytoplankton data by McIntire et al. (this issue), and is also not supported by optical measurements once the pattern of rising attenuation in the early 1980s is placed into a longer time context (Figure 16B). Climate variation is another likely factor to explain changes in blue and UV attenuation, possibly linked through periodic winter upwelling events that are thought to provide the majority of nutrients to phytoplankton each year (Larson et al., 1996a; McManus et al., 1993). Redmond (1999) reported a shift in prevailing winds in the mid-1970s over the region that was associated with the Pacific Decadal Oscillation (PDO, Mantua et al., 1997). The sparse attenuation estimates from proxy data since 1896 fall within the range of the better characterized period since 1978, and from these we conclude that there has been no long-term change in UV transparency since 1896.

UVR Impacts on the Crater Lake Ecosystem

The incident spectrum of sunlight (upper curves in Figure 1A) shows rapid attenuation at the shortest wavelengths because stratospheric ozone strongly absorbs UV-B wavelengths. Figure 13A also shows that summer stratospheric ozone can vary substantially (5-10%) from

year to year. Thus exposure of planktonic organisms to UV-B will depend on atmospheric transparency as well as water column transparency. Because phytoplankton typically control the UVR penetration into the water column, if their growth rates or death rates are influenced by the increasing UV-B that accompanies a decline in ozone, the higher incident UV-B would create a water column that is more transparent to UVR and thus UV-B would penetrate deeper.

The observed correlation of chlorophyll-a with stratospheric ozone (Figure 13B) suggests a direct and significant impact of UV-B on the phytoplankton community. More study of this phenomenon is needed because at this point only two depth ranges (0–30 m and 40–140 m) and one ozone time period (the first 3 weeks of July and of August, averaged) have been investigated. Other controlling factors might have changed in parallel with ozone by coincidence or because the paths of the jet streams influence both ozone and weather. Rain has been suggested as a significant nutrient source for the nitrogen-depleted surface waters (McIntire et al., this issue). Of the three years since 1984 when the 0–30 m chlorophyll-a average for July–August dropped by more than 50% from the preceding year, two of those years (1992 and 2001) were also unusually dry (1992, 66% of average January–June precipitation; 2001, 60% of average).

The stronger correlation between ozone and deep chlorophyll-a compared with shallow chlorophyll-a (Figure 13B) is curious, but the inferred presence of MAAs in near-surface phytoplankton (Figures 12A, 12B), and signs of photoacclimation (Figure 11B) provide the basis for several hypotheses. It is likely that species differ in a variety of ways that would impact their ability to thrive (survive) near the surface of Crater Lake. These include: their sensitivity both to UV-B and to high levels of PAR; their ability to produce MAAs; their cell size (small cells gain less benefit from intracellular compounds that absorb UV-B); and their ability to cope with

scarce nutrients. We hypothesize that phytoplankton living near the surface of Crater Lake are more resistant to UV-B even when ozone levels are high and thus respond less to declines in ozone than phytoplankton at greater depths. Any cells that are growing near their UV-B limits when ozone is high may simply sink faster than their growth rate can replace them when ozone declines. Cells with less UV-B resistance that live deeper in the water column seem more likely to respond in this way. An alternative hypothesis is that cells living near the surface have lower chlorophyll-a concentration per cell (one possible interpretation of Figure 11B), so that a similar percentage reduction in cell abundance in response to an ozone decline would involve a smaller change in chlorophyll-a in the surface waters compared to deeper in the water column.

Other signs of possible UVR impact on the Crater Lake ecosystem include the appearance of UV-resistant organisms and the scarcity or low diversity of organisms in the surface waters of the lake. A previous study reported that phytoplankton diversity and abundance were low in the upper 20 m and only one dominant species has been identified (*Nitzschia gracilis*) representing about 70% of net plankton and nanoplankton in this depth range from 1985–1988 (McIntire et al., 1996). According to McIntire et al. (this issue), *Nitzschia gracilis* is dominant during the stratified summer period in the upper 20 m but the phytoplankton assemblage in the epilimnion also has high densities of smaller species of cyanobacteria (*Aphanocapsa delicatissima* and *Synechocystis sp*.), and lower densities of dinoflagellates *Gymnodinium inversum* and *Peridinium inconspicuum*; the chrysophytes *Dinobryon sertularia* and *D. bavaricum* were good indicators of the lower epiliminon and upper metaliminion, although their mean relative abundance was below 7% of the total cell density.

We hypothesize that the microbial community will respond to UVR stress under the stable shallow-mixing conditions in Crater Lake with the appearance of highly adapted (and thus

UVR resistant) species in the upper 30 m (average $Z_{10\%,320}$=32 m) and moderately resistant species down to 60 m (average $Z_{1\%,320}$=55 m). Urbach et al. (2001) identified two bacterioplankton taxa (CL120-10 verrucomicrobiales and ACK4 actinomycetes) from Crater Lake surface waters that are likely to be resistant to UVR. The deep chlorophyll maximum occurs between 120 and 140 m (Larson et al 1996a), close to the 0.1% depth for PAR (131 m summer average for 1996–2002). The biomass maximum (based on c_{p660}) occurs near the 1% depth for PAR (92 m summer average).

While the scarcity of zooplankton (Larson et al., 1996b) and phytoplankton (McIntire et al., 1996) at depths shallower than 40 m, where UV_{320} is more intense than 5–10% of incident irradiance during summer, is consistent with avoidance or poor survival because of exposure to UVR, other explanations for the phytoplankton distribution are possible. PAR irradiance is more intense than 10% of incident irradiance at depths above 44 m. The diatom *Nitzschia gracilis,* which frequently forms blooms near the surface (McIntire et al., 1996), is probably highly resistant to UVR. Some of our optical data are consistent with the presence of MAA photoprotective compounds in at least part of the phytoplankton community that has become adapted to conditions near the surface (ratio of $K_{d,320}$:$K_{d,380}$ in Figure 6, phytoplankton spectral absorption at 330 nm in Figure 12A, and the ratio of phytoplankton absorption at $a_{p,330}$:$a_{p,675}$ in Figure 12B). Eisner et al., (2003) also found changed *in vivo* particulate absorption spectra ratios that corresponded to changes in phytoplankton pigments (photoprotective versus photosynthetic carotenoids) that were correlated with the light intensity in the water column. Tartarotti et al., (2001) observed a correlation between MAAs in zooplankton (derived from phytoplankton) and elevation in Alpine lakes that they attributed to adaptations providing resistant to UVR exposure.

The absence of higher taxa near the surface of Crater Lake is also likely to be influenced directly or indirectly by UVR although lacking experimental evidence we cannot rule out other factors (grazing, predation, high levels of PAR). A benthic moss (*Drepanocladus aduncas*) has been reported in Crater Lake at depths 25–140 m with the greatest density 40–80 m (McIntire et al., 1994). Analysis of seasonal changes in morphology of this moss might reveal information about growth rate as a function of depth (Riis & Sand-Jensen, 1997) to explore the role of UVR in setting upper and lower depth limits for the population. Small zooplankton (rotifer taxa) have been reported at depths characteristic of moderate UVR but they are scarce above 40 m (Larson et al 1996b). A factor that may influence the distribution of large zooplankton grazers is predator avoidance because the intensity of PAR irradiance at noon on a typical clear summer day exceeds 5 μmol m^{-2} s^{-1} at 100 m and 0.7 μmol m^{-2} s^{-1} at 150 m. Laboratory experiments (summarized in Kalff, 2002) have shown that the distance at which fish can perceive large zooplankton prey becomes limiting at PAR irradiance below 0.6 μmol m^{-2} s^{-1}; more illumination is required to capture smaller prey. Small planktivorous fish and large zooplankton might be forced to stay below an optimal feeding depth in Crater Lake during the day in order to avoid their respective visual predators and then migrate to the zone of maximal phytoplankton abundance at night or twilight to feed. In Crater Lake young Kokanee salmon (taken as prey by rainbow trout) are found near the surface at night but migrate down to 100 m during the day (Buktenica & Larson, 1996). Cladoceran zooplankton migrated diurnally as well, with larger species remaining deeper during the day and night than smaller species. By avoiding visual predators these zooplankton and small fish would also avoid exposure to strong UVR. Some fish are known to use UV-A wavelengths for vision and UV-A may penetrate deeper than visible

wavelengths at dawn and dusk, or whenever the irradiance penetrating the lake surface is dominated by skylight rather than direct rays from the sun (Leech & Johnsen, 2003).

Future Research on UVR in Crater Lake

Future work on UVR in the Crater Lake ecosystem should include experimental manipulations of UVR exposure of Crater Lake organisms (e.g. plankton and moss) to determine sensitivity of survival and productivity at different depths, continuous monitoring of incident UV-B and UV-A radiation, and better monitoring of the optical constituents of the water column that influence UVR penetration, especially in the upper 30 m where it is currently difficult to characterize UV attenuation. Crater Lake is a unique site for investigation of UVR effects on an aquatic ecosystem because it combines unusual UVR transparency with a wide range of depths below the mixed layer where summer exposure to UVR and PAR will be relatively stable from day to day except for the fluctuations in UV-B controlled by stratospheric ozone.

To explore both UV transparency and organic carbon dynamics, a CDOM fluorometer should be added to the suite of sensors in routine CTD profiles, and these data correlated periodically with measurements of particulate absorption spectra and particulate and dissolved organic carbon concentrations for different depths. The ecological control of the microbial community in different depth zones should be explored to clarify the relative importance of stratospheric ozone, nutrient sources (e.g. precipitation versus upwelling), and trophic interactions.

The response of Crater Lake to future climate change will likely involve its sensitivity to the timing and magnitude of changes in precipitation and stratospheric ozone. Precipitation appears to influence UVR transparency through influx of suspended sediments and phytoplankton nutrients. Ozone appears to protect the phytoplankton community from UV-B

radiation, which may allow phytoplankton with moderate UV-B resistance in the upper water column to shield those deeper (and presumably more sensitive) organisms from UVR.

CONCLUSIONS

Crater Lake Color and UVR Transparency

Our recent UVR measurements show that Crater Lake is unusually transparent to UVR and visible wavelengths. In the DNA-damaging UV-B wavelengths diffuse attenuation ranges over values that are similar to, but in some cases more transparent than, other natural waters reported to date. Under average summer conditions (1996–2002) the intensity of a UV-B reference waveband (8-nm waveband centered at 320 nm) at 20 meters was 27% of surface irradiance, and at 40 meters was 5% of surface irradiance (10% at 40 meters under the especially clear conditions in 2001). The lowest UV-B diffuse attenuation coefficients ($K_{d,320}$) were somewhat lower than those reported for the clearest natural waters elsewhere (Lake Vanda, Antarctica, and several oligotrophic ocean regions), and were lower than the previously estimated attenuation by pure water (Smith & Baker, 1981).

Optical Proxies and the Impact of Phytoplankton on UVR Transparency

As in Case 1 marine waters, phytoplankton in Crater Lake normally are the dominant optical attenuator of UVR. During summer the UV attenuation rises from a minimum near the surface to a peak at the deep chlorophyll maximum (DCM) near 120 m. Measurements of $K_{d,UV}$ at different wavelengths parallel each other with increasing depth although only the longer UVR wavelengths can be detected deep in the water column. Optical proxies for UV attenuation include the scattering of light by phytoplankton in the upper part of the photic zone ($c_{p660,}$ measured with a red beam transmissometer), and fluorescence of phytoplankton (F_{chl}, 683 nm) in the deeper regions (75–150 m). Other optical proxies for the depth range 0–40 m include inverse

Secchi depth and diffuse attenuation in the broad blue waveband (400–500 nm), corresponding to historical underwater measurements with blue filter photometers. Only during rare heavy rains in summer does the optical dominance of phytoplankton give way to an optical signal from light scattering by suspended mineral particles and a likely breakdown of the proxy relationships. Excluding occasional wet summer months, $K_{d,UV}$ derived from Secchi depth was correlated with phytoplankton biomass as measured by chlorophyll-a concentration for the period 1984–2002.

UVR Impact on the Crater Lake Ecosystem

In the absence of UVR experiments the impact of UVR on lake biota can be inferred only from correlations. Since 1984 the summer average stratospheric ozone over Crater Lake was correlated with chlorophyll-a concentration in the photic zone (for depth ranges 0–30 m and 40–140 m), suggesting a direct or indirect impact of UV-B radiation on Crater Lake phytoplankton. Particulate absorption at a wavelength typical of UV-B protective pigments in phytoplankton varied with depth in proportion to UV-B exposure. Few planktonic organisms appear in the upper water column where daily exposure to UV-B irradiance is stronger than 5–10% of surface irradiance. Phytoplankton at depths where irradiance levels were stronger than 1% of incident UV-B and 15% of incident PAR developed maximal photoacclimation to strong sunlight. Visible light penetration at noon should become limiting at about 150 m for fish visual predation upon large zooplankton. Diurnal migration of small fish and large zooplankton sufficient to avoid visual predators would also prevent their exposure to strong UVR.

Long-term Trends and Possible Impacts of Future Climate Change

Our comparisons of nearly-continuous annual summer optical data since 1978 suggest that UV transparency changes on decadal and longer cycles, perhaps in response to a combination of rain and stratospheric ozone influencing the phytoplankton community, with

heavy summer rain occasionally influencing the level of suspended mineral particles. We also cannot rule out the impact of trophic interactions and nutrient upwelling as additional factors influencing phytoplankton and UV transparency. The sparse attenuation estimates from proxy data between 1896 and 1978 fall within the range of the better characterized period since 1978, and from these we infer that there has been no long-term change in UV transparency since 1896.

ACKNOWLEDGEMENTS

We are grateful to John Morrow and Michael Holas of Biospherical Instruments, Inc. who provided profiling instruments for spectral radiance reflectance measurements in Figure 2 and for comparison measurements of UV irradiance and $K_{d,\lambda}$ in Figure 4. Valuable comments were also provided by Emmanuel Boss and two anonymous reviewers.

REFERENCES CITED

Ayoub, L. M., B. R. Hargreaves & D. P. Morris, 1996. UVR attenuation in lakes: Relative contribution of dissolved and particulate material. SPIE Ocean Optics XIII 2963: 338–343.

Bacon, C. R., J. V. Gardner, L. A. Mayer, M. W. Buktenica, P. Dartnell, D. W. Ramsey & J. E. Robinson, 2002. Morphology, volcanism, and mass wasting in Crater Lake, Oregon. Geological Society of America Bulletin 114.6: 675–692.

Baker, K. S. & R.C. Smith, 1979. Quasi-inherent characteristics of the diffuse attenuation coefficient for irradiance. Ocean Optics VI, SPIE 208: 60–63.

Barnard, G. P., 1938. The spectral sensitivity of selenium rectifier photoelectric cells. Proceedings of the Physical Society 51: 222–236.

Belzile, C., W. F. Vincent & M. Kumagai, 2002. Contribution of absorption and scattering to the attenuation of UV and photosynthetically available radiation in Lake Biwa. Limnology and Oceanography 47: 95–107.

Biospherical Instruments, 1998. GUV data processing and quality control procedures, C. Version 13, October 1998. Biospherical Instruments, Inc., San Diego, California, USA.

Bishop, J. K. B., 1986. The correction and suspended particulate matter calibration of SeaTech transmissometer data. Deep-Sea Research 33: 121–134.

Boss, E. S., R. W. Collier, G. L. Larson, K. Fennel & W. S. Pegau, this issue. Measurements of spectral optical properties and their relation to biogeochemical variables and processes in Crater Lake, Crater Lake National Park, OR.

Bricaud, A., A. Morel & L. Prieur, 1981. Absorption by dissolved organic matter in the sea (yellow substance) in the UV and visible domains. Limnology and Oceanography 26: 43–53.

Buktenica, M. W. & G. L. Larson, 1996. Ecology of Kokanee salmon and rainbow trout in Crater Lake, Oregon, Journal of Lake and Reservoir Management 12: 298–310.

Coblentz, W. W. & R. Stair, 1936. The evaluation of ultra-violet solar radiation of short wave-lengths. Proceedings of the National Academy of Science 22: 229–233.

Davies-Colley, R. J., 1988. Measuring water clarity with a black disk, Limnology and Oceanography 33: 616–623.

Dierssen, H. M. & R. C. Smith, 2000. Bio-optical properties and remote sensing ocean color algorithms for Antarctic Peninsula waters. Journal of Geophysical Research 105: 26,301–26,312.

Diller, J. S., 1897. Crater Lake, Oregon. National Geographic Magazine 8: 33–48 (cited in Larson et al., 1996a)

Eisner, L. B., M. S. Twardowski, T. J. Cowles & M. J. Perry, 2003. Resolving phytoplankton photoprotective:photosynthetic carotenoid ratios on fine scales using in situ special absorption measurements. Limnology and Oceanography 48: 632–646.

Fennel, K. & E. Boss, 2003. Subsurface maxima of phytoplankton and chlorophyll: Steady-state solutions from a simple model. Limnology and Oceanography 48: 1521–1534.

Goldman, C. R., D. T. Mason & J. E. Hobbie, 1967. Two antarctic desert lakes. Limnology and Oceanography 12: 295–310.

Gordon, H. R., 1989. Can the Lambert-Beer law be applied to the diffuse attenuation coefficient of ocean water? Limnology and Oceanography 34:1389–1409.

Gordon, H. R., 1999. Contribution of Raman scattering to water-leaving radiance: a reexamination. Applied Optics 38: 3166–3174.

Haltrin, V. I., G. W. Kattawar & A. D. Weidman, 1997. Modeling of elastic and inelastic scattering effects in oceanic optics. SPIE 2963: 597–602.

Hargreaves, B. R., 2003. Water Column Optics and Penetration of UVR. In E. W. Helbling & H. E. Zagarese (eds), UV Effects in Aquatic Organisms and Ecosystems, Comprehensive Series in Photochemical and Photobiological Sciences. Royal Society of Chemistry, Cambridge, UK: 59–105.

Helbling, E. W., V. Villafañe & O. Holm-Hansen, 1994. Effects of ultraviolet radiation on Antarctic marine phytoplankton photosynthesis with particular attention to the influence of mixing. In C. S. Weiler & P. A. Penhale (eds), Ultraviolet Radiation In Antarctica: Measurements and Biological Effects, Antarctic Research Series, Vol. 62. American Geophysical Union, Washington D.C.: 207–227.

Hewes C. D., B. G. Mitchell, T. A.Moisan, M. Vernet & F. M. H. Reid, 1998. The phycobilin signatures of chloroplasts from three dinoflagellate species: A microanalytical study of Dinophysis caudata, D-fortii, and D-acuminata (Dinophysiales, Dinophyceae). Journal of Phycology 34: 945–951.

Højerslev, N. K., 1994. A history of early optical oceanographic instrument design in Scandinavia. In R.W. Spinrad, K.L. Carder, M.J. Perry (eds), Ocean Optics. Oxford Univ. Press, New York: 118–147

Højerslev, N. K. & T. Aarup, 2002. Optical measurements on the Louisiana shelf off the Mississippi River. Estuarine and Coastal Shelf Science 55: 599–611.

Jassby, A. D., C. R. Goldman, J. E. Reuter & R. C. Richards, 1999. Origins and scale dependence of temporal variability in the transparency of Lake Tahoe, California-Nevada. Limnology and Oceanography 44: 282–294.

Jerlov, N. G., 1950. Ultra-violet Radiation in the Sea. Nature 166: 111–112.

Johnson (=Jerlov), N. G., 1946. On anti-rachitic ultra-violet radiation in the sea. Medd. Oceanogr. Inst. Gothenburg. Ser. B. 3: 11 (cited in Højerslev 1994).

Kalff, J., 2002. Limnology: inland water ecosystems. Prentice Hall, 592 p.

Kirk, J. T. O., 1994a. Optics of UV-B radiation in natural waters. Archiv für Hydrobiologie Beihefte Ergebnisse der Limnologie 43:71–99.

Kirk, J. T. O., 1994b. Light & Photosynthesis in Aquatic Ecosystems, 2nd ed. Cambridge University Press, Cambridge.

Kirk, J. T. O., B. R. Hargreaves, D. P. Morris, R. Coffin, B. David, D. Frederickson, D. Karentz, D. Lean, M. Lesser, S. Madronich, J. H. Morrow, N. Nelson & N. Scully, 1994. Measurement of UV-B radiation in two freshwater lakes: an instrument intercomparison. Archiv für Hydrobiologie Beihefte Ergebnisse der Limnologie 43: 71–99.

Larson, D. W., 1972. Temperature, Transparency, and phytoplankton productivity in Crater Lake, Oregon. Limnology and Oceanography 17:410–417.

Larson, D. W., 2002. Probing the Depths of Crater Lake, American Scientist., 90:64–71.

Larson, G. L., C. D. McIntire, M. Hurley & M. W. Bukenica, 1996a. Temperature, Water Chemistry, and Optical Properties of Crater Lake. Journal of Lake and Reservoir Management 12: 230–247.

Larson, G. L., C. D. McIntire, R. E. Truitt, M. W. Buktenica & E. Karnaugh-Thomas, 1996b. Zooplankton Assemblages in Crater Lake, Oregon, USA. Journal of Lake and Reservoir Management 12: 281–297.

Laurion, I., M. Ventura, J. Catalan, R. Psenner & R. Sommaruga, 2000. Attenuation of ultraviolet radiation in mountain lakes: factors controlling the among- and within-lake variability. Limnology and Oceanography 45: 1274–1288.

Laurion, I., F. Blouin, S. Roy, 2003. The quantitative filter technique for measuring phytoplankton absorption: Interference by MAAs in the UV waveband. Limnology and Oceanography: Methods 1: 1–9.

Leech, D. M. & S. Johnsen, 2003. Behavioral responses—UVR avoidance and vision. pp. In E.W. Helbling & H. E. Zagarese (eds), UV Effects in Aquatic Organisms and Ecosystems, Comprehensive Series in Photochemical and Photobiological Sciences. Royal Society of Chemistry, Cambridge, UK: 455–484.

Lohrenz, S. E., 2000. A novel theoretical approach to correct for pathlength amplification and variable sampling loading in measurements of particulate spectral absorption by the quantitative filter technique. Journal of Plankton Research 22: 639–657.

MacIntyre, H. L., T. M. Kana, T. Anning & R. J. Geider, 2002. Photoacclimation of photosynthesis irradiance response curves and photosynthesis pigments in microalgae and cyanobacteria. Journal of Phycology 38: 17–38.

Madronich, S. 1993. UV radiation in the natural and perturbed atmosphere. In M. Tevini (ed), UVB Radiation and Ozone Depletion: Effects on Humans, Animals, Plants, Micro-organisms, and Materials. CRC Press, Boca Raton, Florida: 17–69

Mantua, N. J., S. T. Hare, Y. Zhang, J. M. Wallace & R. C. Francis, 1997. A Pacific interdecadal climate oscillation with impacts on salmon production. Bulletin of the American Meteorological Society 78: 1069–1079.

Markager, S. & W. F. Vincent, 2000. Spectral light attenuation and the absorption of UV and blue light in natural waters. Limnology and Oceanography 45: 642–650.

McIntire, C. D., H. K. Phinney, G. L. Larson & M. Buktenica, 1994. Vertical distribution of a deep-water moss and associated epiphytes in Crater Lake, Oregon. Northwest Sciences 68: 11–21.

McIntire, C. D., G. L. Larson, R. E. Truitt & M. K Debacon, 1996. Taxonomic structure and productivity of phytoplankton assemblages in Crater Lake, Oregon. Lake and Reservoir Management 12: 259–280.

McIntire, C. D., G. L Larson & R. E. Truitt, this issue. Taxonomic composition and production dynamics of phytoplankton assemblages in Crater Lake, Oregon.

McManus, J., R. W. Collier & J. Dymond, 1993. Mixing processes in Crater Lake, Oregon. Journal of Geophysical Research, 98: 18295–18307.

Mitchell, B.G., 1990. Algorithms for determining the absorption coefficient of aquatic particulates using the quantitative filter technique (QFT). Ocean Optics X, SPIE 1302: 137–148.

Morel, A., 1974. Optical Properties of pure water and pure sea water. In N. G. Jerlov & E. Steelmann Nielsen (eds), Optical Aspects of Oceanography. Academic Press, New York: 1–24.

Morel, A. & S. Maritorena, 2001. Bio-optical properties of oceanic waters: A reappraisal. Journal of Geophysical Research, 106: 7163–7180.

Morel, A. & L. Prieur, 1977. Analysis of variations in ocean color. Limnology and Oceanography, 22: 709–722.

Patterson, K. W., R. C. Smith & C. R. Booth, 1997. A method for removing a majority of the error in PUV attenuation coefficients due to spectral drift in response with depth in the water column. Ocean Optics XIII, SPIE 2963: 737–742.

Pegau, W. S., D. Gray & J. R. V. Zaneveld, 1997. Absorption and attenuation of visible and near-infrared light in water: dependence on temperature and salinity. Applied Optics 36: 6035–6046.

Pettit, E., 1936. On the color of Crater Lake water. Proceedings of the National Academy of Sciences of the United States of America 22: 139–146.

Pienitz, R. & W. F. Vincent, 2000. Effect of climate change relative to ozone depletion on UV exposure in subarctic lakes. Nature 404.6777: 484–487.

Pope, R. M. & E. S. Fry, 1997. Absorption spectrum (380–700 nm) of pure water. II. Integrating cavity measurements. Applied Optics 36: 8710–8723.

Preisendorfer, R. W., 1986. Secchi disk science: visual optics of natural waters. Limnology and Oceanography 31: 909–926.

Redmond, K. T., 1999. Crater Lake Evaporation and Climate Variability. Project report for subcontract No. B0023A-01.

Riis, T. & K. Sand-Jensen, 1997. Growth reconstruction and photosynthesis of aquatic mosses: influence of light, temperature and carbon dioxide at depth. Journal of Ecology 85: 359–372.

Sathyendranath, S, L. Lazzara & L. Prieur, 1987. Variations in the spectral values of specific absorption of phytoplankton. Limnology & Oceanography 32: 403–415.

Schindler, D. W. & P. J. Curtis, 1997. The role of DOC in protecting freshwaters subject to climatic warming and acidification from UV exposure. Biogeochemistry 36: 1–8.

Sharp, J. H., R. Benner, L. Bennett, C. A. Carson, R. Dow & S. E. Fitzwater, 1993. Re-evaluation of high temperature combustion and chemical oxidation measurements of dissolved organic carbon in seawater. Limnology and Oceanography 38: 1174–1782.

Smith, R. C. & J. E. Tyler, 1967. Optical Properties of Clear Natural Waters. Journal of the Optical Society of America 57: 589–595.

Smith, R. C., J. E. Tyler & C. R Goldman, 1973. Optical properties and color of Lake Tahoe and Crater Lake. Limnology and Oceanography 18:189–199.

Smith, R. C. & J. E. Tyler, 1976. Transmission of solar radiation into natural waters. In K.C. Smith (ed.), Photochemical and Photobiological Reviews, Vol. 1, Plenum Press, New York,: 117–156

Smith, R. C. & K. S. Baker, 1981. Optical Properties of the clearest natural waters (200–800 nm). Applied Optics 20: 177–184.

Sommaruga, R., 2001. The role of solar UV radiation in the ecology of alpine lakes. Journal of Photochemistry & Photobiology, B: Biology 62: 35–42.

Sosik, H. M., 1999. Storage of marine particulate samples for light-absorption measurements. Limnology and Oceanography 44: 1139–1141.

Tyler, J. E. & R. W Presiendorfer, 1962. Transmission of energy within the sea. In M.N. Hill (ed.), The Sea, Vol. 1. Interscience, New York (cited in Tyler & Smith 1976): 397–451

Tyler, J. E., 1965. In situ spectroscopy in ocean and lake waters. Journal of the Optical Society of America 55: 800–805.

Tyler, J. E., 1968. The Secchi Disc. Limnology and Oceanography 13: 1–6.

Tyler, J. E. & R. C. Smith, 1970. Measurements of Spectral Irradiance underwater. Gordon and Breach Science Publishers, New York.

Tartarotti, B., I. Laurion & R. Sommaruga, 2001. Large variability in the concentration of mycosporine-like amino acids among zooplankton from lakes located across an altitude gradient. Limnology and Oceanography 46: 1546–1552.

Utterback, C. L., L. D. Phifer & R. J. Robinson, 1942. Some Chemical, Planktonic, and Optical Characteristics of Crater Lake. Ecology 23: 97–103.

Vincent, W. F., R. Rae, I. Laurion, C. Howard-Williams & J. C. Priscu, 1998. Transparency of Antartctic ice-covered lakes to solar UV radiation. Limnology and Oceanography 43: 618–624.

Yentsch, C. S. & D.A. Phinney, 1989. A bridge between ocean optics and microbial ecology. Limnology and Oceanography 34: 1694–1705.

Zaneveld, J. R. & R. Bartz, 1984. Beam attenuation and absorption meters. SPIE Ocean Optics VII 486: 318–324.

Zaneveld, J. R. V. & W. S. Pegau, 2003. Robust underwater visibility parameter. Optics Express Vol. 11: 2997–3000.

Zaneveld, J. R. V., E. Boss & A. Barnard, 2001. Influence of surface waves on measured and modeled irradiance profiles. Applied Optics 40: 1442–1449.

Table 1. Average diffuse attenuation coefficients and % attenuation of E_d (1996–2002) by depth.

K_d Depth (m)	E_d Depth(m)	$K_{d,320}$ (m^{-1})	2SE	$E_d\%_{320}$	$K_{d,380}$	2SE	$E_d\%_{380}$	$K_{d,blue}$	2SE	$E_d\%_{blue}$	K_{dPAR}	$E_d\%_{PAR}$
2.8	5.0	0.062	0.0054	73%	0.027	0.0049	88%	0.027	0.0036	87%	0.108	58%
7.3	10.0	0.064	0.0056	53%	0.028	0.0045	76%	0.028	0.0048	76%	0.066	42%
12.2	15.0	0.066	0.0055	38%	0.029	0.0036	66%	0.026	0.0040	67%	0.050	33%
17.5	20.0	0.074	0.0086	27%	0.032	0.0041	56%	0.028	0.0035	58%	0.048	26%
22.5	25.0	0.081	0.0089	18%	0.037	0.0050	47%	0.033	0.0045	49%	0.047	20%
27.5	30.0	0.084	0.0090	12%	0.037	0.0051	39%	0.031	0.0041	42%	0.044	16%
32.7	35.0	0.088	0.0081	7.5%	0.039	0.0048	32%	0.034	0.0048	36%	0.045	13%
37.7	40.0	0.091	0.0069	4.7%	0.040	0.0043	26%	0.034	0.0034	30%	0.045	10%
42.5	45.0	0.097	0.0058	2.9%	0.045	0.0033	21%	0.037	0.0035	25%	0.047	8.2%
47.5	50.0	0.103	0.0072	1.7%	0.047	0.0036	16%	0.038	0.0028	21%	0.048	6.5%
54.8	60.0	0.103	0.0065	0.62%	0.049	0.0037	10%	0.040	0.0028	14%	0.043	4.2%
64.5	70.0	0.113	0.0075	0.20%	0.052	0.0032	5.9%	0.043	0.0025	9.0%	0.045	2.7%
74.3	80.0	*0.122*		0.059%	0.056	0.0049	3.4%	0.045	0.0040	5.7%	0.047	1.7%
84.3	90.0	*0.134*		0.016%	0.062	0.0050	1.8%	0.050	0.0044	3.5%	0.051	1.0%
94.3	100.0				0.065	0.0045	1.0%	0.053	0.0035	2.0%	0.053	0.59%
104.7	110.0				0.068	0.0044	0.48%	0.055	0.0032	1.2%	0.055	0.34%
115.0	120.0				0.073	0.0046	0.23%	0.059	0.0029	0.65%	0.060	0.19%
125.0	130.0				0.073	0.0045	0.11%	0.059	0.0038	0.36%	0.059	0.10%
135.0	140.0				0.073	0.0059	0.054%	0.058	0.0040	0.201%	0.058	0.058%
145.0	150.0				0.065	0.0071	0.028%	0.052	0.0031	0.120%	0.052	0.034%
155.0	160.0				0.056	0.0047	0.016%	0.047	0.0027	0.075%	0.048	0.021%
164.6	170.0							0.044	0.0046	0.048%	0.044	0.014%
173.6	180.0							0.040	0.0061	0.032%	0.040	0.0092%

FIGURE CAPTIONS

Figure 1. A. Crater Lake solar irradiance spectra (304–750 nm) at depths 20–160 m, 20 August 2001 (air scan 12:04 PDT). LI-COR LI-1800uw spectroradiometer (8 nm bandwidth; cosine response to downwelling irradiance). Incident E_d irradiance (thick line) plotted along with model E_o irradiance (thin line, distinct from the measurements only at the lowest and highest wavelengths) from RTBasic (Biospherical Instruments; 8-stream option, 2 nm bandwidth; model output adjusted using 8 nm running averages of model Log (E_d) to account for the 8 nm bandwidth of the LI-1800uw data; ozone=313 DU from satellite; P_{atm}=774 torr from elevation). Ratios of measured:modeled data averaged 98% for 308–800 nm, and 96% for 308–400 nm (range 87–109%). **B.** Attenuation depths (10% and 1%) from spectral irradiance in Figure 1A. For PAR, $Z_{10\%}$=50m, $Z_{1\%}$=100 m, $Z_{0.1\%}$=140 m. For UV-B (320 nm), $Z_{10\%}$=37 m, $Z_{1\%}$=62 m. Polynomial regressions fitted to the points: $Z_{10\%} = 4.9534E\text{-}07 \cdot WL^4 - 7.6076E\text{-}04 \cdot WL^3 + 4.3388E\text{-}01 \cdot WL^2 - 1.0855E+02 \cdot WL^1 + 1.0082E+04$; $Z_{1\%} = 8.2806E\text{-}07 \cdot WL^4 - 1.2583E\text{-}03 \cdot WL^3 + 7.0974E\text{-}01 \cdot WL^2 - 1.7559E+02 \cdot WL^1 + 1.6128E+04$.

Figure 2. A. Crater Lake upwelling irradiance, 20 August 2001 (Biospherical Instruments PRR-800 reflectance profiler lowered inverted, units $\mu W\ cm^{-2}\ nm^{-1}$). Depth (m) is indicated in the legend. Peak near 400 nm is source of deep blue color when viewed from above. Red peak is fluorescence from phytoplankton (683 nm). **B.** Crater Lake radiance reflectance, 20 August 2001 (Biospherical Instruments PRR_800, data binned at 1m intervals). Near the surface the spectrum is similar to upwelling irradiance. At greater depths the reflectance in UV and blue wavelengths declines because absorbance coefficients increase with depth faster than backscatter coefficients. At longer wavelengths the signal rises with increasing depth because Raman scatter and phytoplankton fluorescence (Chlorophyll-a at 683 nm and for 120 & 150 m depths, possibly phycoerythrin at 589 nm) increase rapidly in the upwelling radiance signal relative to downwelling irradiance.

Figure 3. Crater Lake spectral diffuse attenuation from spectral irradiance in Figure 1, plus an average for 10–18 m depth calculated from profiles by PRR-800 and PUV-2500 instruments from Biospherical Instruments, Inc. (BSI). LI-1800uw K_d was calculated for each depth interval

and then averaged for a range of depths (error bars are +/-S.E. of mean for depth ranges included in mean). BSI K_d was calculated for 10–18 m from polynomial regressions of $E_{d,Z}$ vs depth to reduce noise from surface reflections. Note that the minimum K_d was at 412 nm. Values for wavelengths longer than 560 nm are excluded below 40 m because of Raman scatter artifact described in Figure 2B. Shorter UV wavelengths are excluded at depths below 55 m because of instrument detection limits. The lowest $K_{d,320}$ value was 0.057 m^{-1} (PUV-2500, 10–18m).

Figure 4. K_d versus depth for selected wavelengths in Crater Lake (20 August 2001) showing minimum values at surface and increasing values with depth to the deep chlorophyll maximum (DCM). Four wavebands and three instruments are compared (smoothed with 8 m running averages above 60 m). Narrow-band signals show parallel changes with depth while the PAR waveband increases near the surface (where highly-attenuated red wavelengths are detected). BSI instruments (PUV-2500, solid circles; PRR-800, solid triangles) give similar results to LI-COR LI-1800uw (open circles) except for greater noise in the latter near the surface because of long scan times. The 320 nm curve for LI-1800uw data was limited to about 75 m because of instrument sensitivity but the PUV-2500 was only lowered to 63 m. The PRR-800 radiometer was not equipped with a 320 nm sensor during this comparison and the PUV-2500 PAR signal is not included for greater clarity. The optically-mixed depths correspond to the thermally mixed epilimnion (0–10 m, not shown). The lowest $K_{d,320}$ averages were 0.057 m^{-1} (PUV-2500, 10–18m) and 0.058 m^{-1} (LI-1800uw, 0–20 m).

Figure 5. Average K_d for three wavebands versus depth in Crater Lake (June–September 1996–2002, LI-1800uw data, N=15 dates, bars indicate +/- S.E.) showing the summer pattern with minimum K_d at the surface and maximum K_d at the deep chlorophyll maximum (DCM). $K_{d,blue}$ was calculated for the irradiance waveband 400–500 nm while $K_{d,320}$ and $K_{d,380}$ were calculated using the average from 2 nm above to 2 nm below the central wavelength. The average value for $K_{d,320}$ near the surface (0–5 m) was 0.062 m^{-1}.

Figure 6. Crater Lake K_d ratios from data in Figure 5 (June–September 1996–2002, LI-1800uw). Least squares regression for $K_{d,320}$:$K_{d,380}$ versus depth (m), $y = -0.0031x + 2.32$, r^2=0.68. Average 0–10 m ratios: $K_{d,320}$:$K_{d,blue}$, 2.28 (SE=0.007), $K_{d,380}$:$K_{d,blue}$, 0.98 (SE=0.002),

$K_{d,320}$:$K_{d,380}$ = 2.32 (SE = 0.012). Average 0–40 m ratios: $K_{d,320}$:$K_{d,blue}$ = 2.52 (SE=0.058); $K_{d,380}$:$K_{d,blue}$ = 1.11 (SE=0.029); $K_{d,320}$:$K_{d,380}$ = 2.27 (SE = 0.016).

Figure 7. A. Seasonal pattern of $K_{d,320}$ in Crater Lake, 1996–2002 (averaged 0–40 m). Typically the minimum K_d occurred in July or August. The highest K_d values during this period were in 1998–1999, the lowest in 2001. **B.** Interannual variation in $K_{d,380}$ for three depths, July–August average, 1996–2002. Little change occurred at the depth of the deep chlorophyll maximum (100–140 m). Larger variations occurred for depths 0–20 m and 20–40 m, which showed similar changes in 6 out of 7 years. Error bars (+/- 1 S.E.) are shown for years with multiple measurements (N=2, 1996, 1998, 1999, 2002; N=3, 2001).

Figure 8. A. Crater Lake particulate organic carbon (POC, C g m^{-3}) versus depth, 1999. POC was derived from 2 m binned c_{p660} data (SeaTech transmissometer). Calculation: POC = (cp660+0.024-X)/0.032)/83.3 (proxy equation from Boss et al., this issue, but X was adjusted on each date to match POC over 300–500 m for all dates). Photic zone particulate carbon appears to increase over the course of the summer. **B.** Crater Lake Total Organic Carbon (TOC) versus depth, 1999. TOC (carbon g m^{-3}) in whole water samples was determined from three analytical replicates with a Shimadzu TOC-5000 (error bars are +/- S.E.). **C.** Crater Lake Dissolved Organic Carbon (DOC) versus depth, 1999. DOC calculated by difference (TOC-POC). Because no replicate samples were collected and analytical replicates for TOC were noisy, only the values above 200 m are plotted. DOC concentration appears to peak near 80 m, and to increase in the photic zone from July through September, consistent with a summer increase in CDOM observed in 2001 by Boss et al. (this issue).

Figure 9. A. Crater Lake c_{p660} versus depth for 1995. Unusually high values near surface and deep in the water column are probably suspended mineral particles from storm runoff. The broad peak centered at 70 m is normal (assumed to be microbial biomass). Rain record at Crater Lake NPS Headquarters: 4–19 June = 4.7", 6–12July = 3.8", 25July = 0.9". Snow pack also melted late this year (5 July 1995). **B.** Crater Lake turbidity (c_{p660}) reached unusual levels during summer 1995 compared to 1994 (a typical year), coincident with high precipitation and runoff during Spring and Summer 1995 (see caption for Figure 10A). Both the surface and deep water

(averages for 0–20 m and 300 m plotted) were elevated in early July and went much higher at the surface during the days after the 25 July thunderstorm and appears to have reached the bottom 2–4 weeks after the storm.

Figure 10. A. Crater Lake rain (inches per month at Crater Lake NPS Headquarters) and chlorophyll-a (0.45 um filter), averaged 0–30 m and 40–140 m (1984–2002 July–August). **B.** Crater Lake $K_{d,320}$ (10–40 m) versus surface Chl-*a* (0–30 m, retained on0.45 micron filter) for July and August 1984–2002. Only "dry" months and several months with heavy but frozen precipitation are included in the regression. Regression equation for warm dry months, $y = 0.15x + 0.08$ ($r^2 = 0.44$).

Figure 11. A. Crater Lake empirical model for $K_{d,380}$ versus depth based on bio-optical signals (20 August 2001). Temperature and depth from Seabird CTD; chlorophyll fluorescence (F_{chl}, relative units) from Wetlabs WetStar fluorometer; c_{p660} from SeaTech transmissometer (c_w=0.411 m^{-1}); $K_{d,380}$ (open circles) from LI-1800uw scans. Model: $K_{d,380}= 0.40*F_{chl} + 0.36*c_{p660}$. **B.** Crater Lake phytoplankton photoacclimation index for 2001 (from ratio of bio-optical signals, F_{chl}:c_{p660}).

Figure 12. A. Crater Lake particulate absorption (a_p) spectra from 5 depths (20 August 2001). QFT method as modified by Lohrenz (2000) using GF/F filters (0.5–1.0 liters filtered); filter supported on quartz disc and scanned using a Shimadzu 160-UV spectrophotometer. Chlorophyll-a absorption peaks at 675 nm and 430 nm; apparent micosporine-like amino acid (MAA) peak at 325 nm (arrow) clearly visible in 25 m and 50 m samples. Chlorophyll-a concentrations calculated from 675 nm peaks (0.038–0.38 mg m^{-3} using ap^*_{675}=0.040) closely match the [Chlorophyll-a] calculated from data in Figure 3 using the diffuse attenuation model of Morel and Maritorena 2001. Typical ap^*_{675} = 0.035 according to Sathyendranath et al. (1987). **B.** Absorption ratios consistent with photoprotection from UV-B in phytoplankton near the surface (MAA peak versus Chlorophyll-a red peak ratio follows attenuation trend for UV-B irradiance; Chlorophyll-a blue peak versus Chlorophyll-a red peak ratio remains constant with depth). Ratio of F_{chl}:c_{p660} shows photoacclimation as in Figure 11B.

Figure 13. A. Crater Lake surface Chlorophyll-a (0–30 m average and 40–140 m average, retained on 0.45 micron filter) for July and August 1984–2002, and stratospheric ozone over Crater Lake during July and August (average of day 1–17 each month for latitude +43, longitude -122, source Nimbus-7 TOMS sensor, 1978–93, Earth Probe TOMS sensor, 1993–present, http://toms.gsfc.nasa.gov/teacher/ozone_overhead_archive_V8.html). **B.** Chlorophyll-a (1984–2002 averages for July & August, 0–30 m and 40–140 m retained on 0.45 micron filter) versus Stratospheric ozone (DU) averaged for first 17 days of the sample month (see Figure 13A for source). Regression equation for deep [Chlorophyll-a], $y = 0.025x - 7.45$ ($r^2 = 0.49$); for shallow [Chlorophyll-a], $y = 0.0037x - 1.07$ ($r^2 = 0.27$).

Figure 14. A. Regressions show that Crater Lake $K_{d,320}$ and $K_{d,380}$ can be calculated from $K_{d,blue}$ (400–500 nm) using data averaged over 0–40 m for July–August 1996–2002: $K_{d,320} = 1.65 * K_{d,blue} + 0.027$, $r^2=0.66$; $K_{d,380} = 1.16 * K_{d,blue} - 0.001$, $r^2=0.92$. **B.** Time series for $K_{d,320}$ and $K_{d,380}$ (0–40 m) in Crater Lake using direct radiometer measurements (1966, 1969, 1996–2002) and proxy derived from $K_{d,blue}$ using blue-filter photometer data, (1940, 1969, 1980–1991). For 1966 $K_{d,380}$ was estimated from reported $E_{d,360–390nm}$ vs depth (5–25m) yielding $K_{d,380}=0.024$; after adjustment for 0–40 m depth range using recent patterns of K_d versus depth (Figures 5 & 6), $K_{d,380}= 0.027$. For 1966 and 1969 the $K_{d,320}$ radiometer data were estimated from measured radiometer $K_{d,380}$ using $K_{d,320} = K_{d,380}$ *

Figure 15. A. Crater Lake regression of photometer $K_{d,blue}$ against inverse Secchi depth (units m^{-1}; annual averages for only same-day measurements, 1968–1991). Equation: $K_{d,blue} = 2.08/Z_{SD} – 0.026$ ($r^2=0.54$, N=13 years). **B.** Crater Lake time series of $K_{d,blue}$ from direct photometer (gray circles) and radiometer (black circles) measurements and proxy using Secchi depth (open circles). The spike in 1995 follows heavy summer rain in June and July (see Figure 10A). Many of the comparison points are for measurements made on different days in the same month.

Figure 16. A. Crater Lake time series (1940–2002) of $K_{d,320}$ and $K_{d,380}$ using radiometer and photometer data from Figure 15B plus all valid Secchi disk data. Open symbols are from Secchi disk (triangles are $K_{d,320}$, squares are $K_{d,380}$); black symbols are direct from radiometer; light gray

symbols are photometer data; dark gray triangles are $K_{d,320}$ derived from radiometer $K_{d,380}$. The spike in 1995 follows heavy rain in June and July. **B.** Crater Lake times series of $K_{d,320}$ using average of all sources of data. Sample frequency prior to 1978 is inadequate to characterize cycles but maximum and minimum values from 1896–1969 (0.07–0.12) fall within the same range as the more frequent measurements since 1978 (0.07–0.14, or 0.07–0.12 without including the rainy summer of 1995).

Figure 1A.

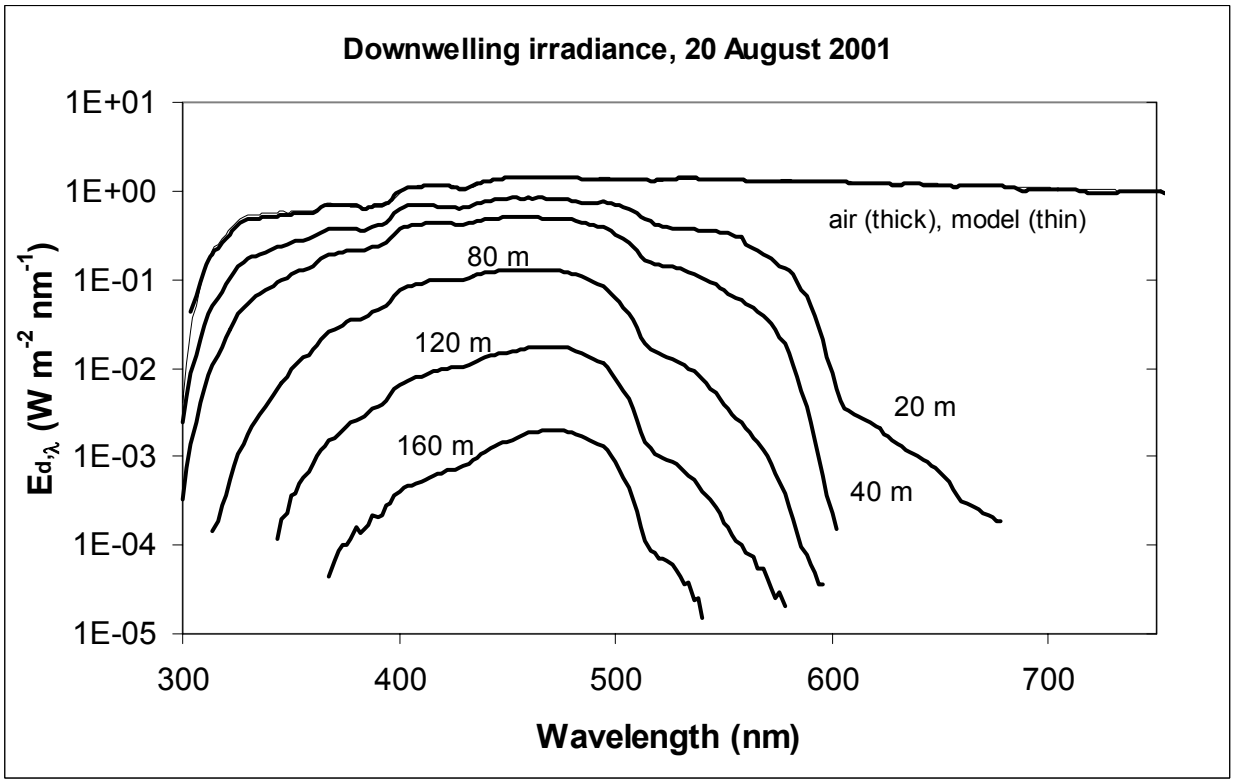

Figure 1B.

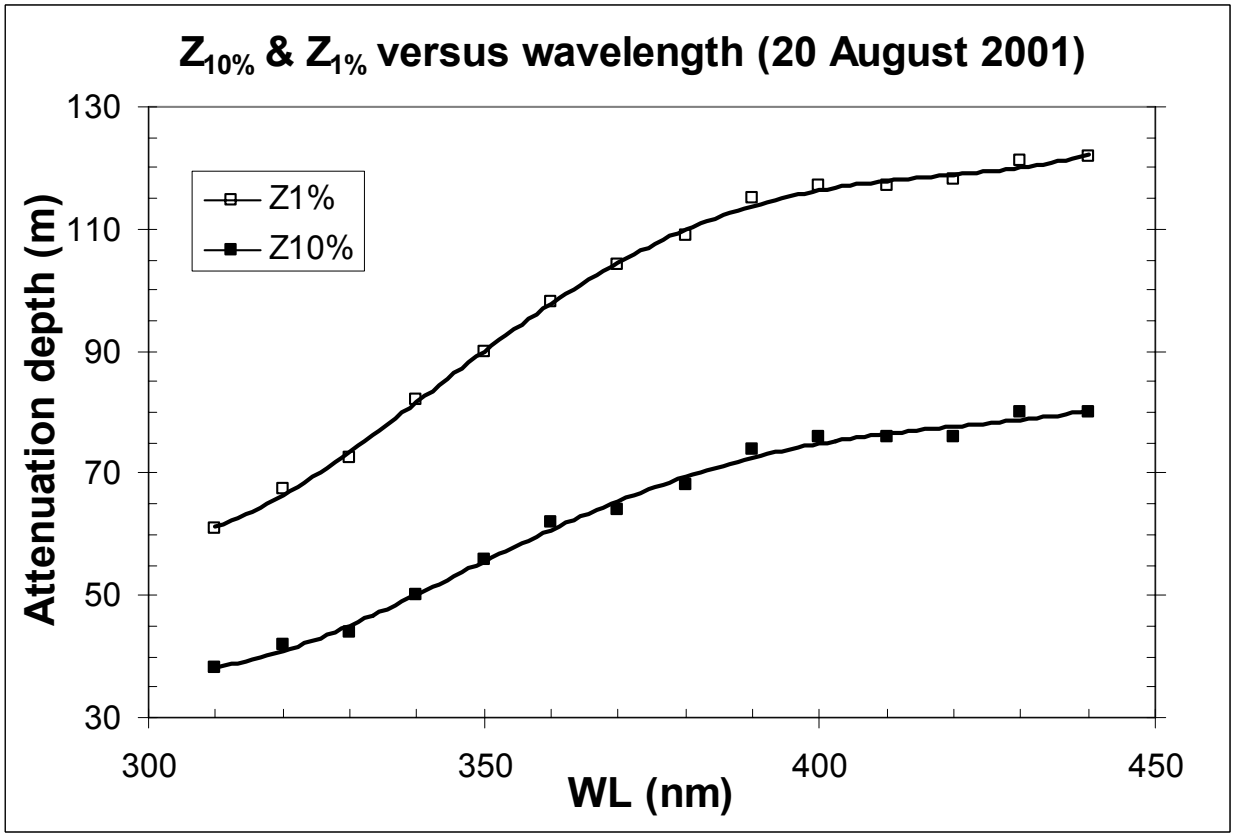

Figure 2A.

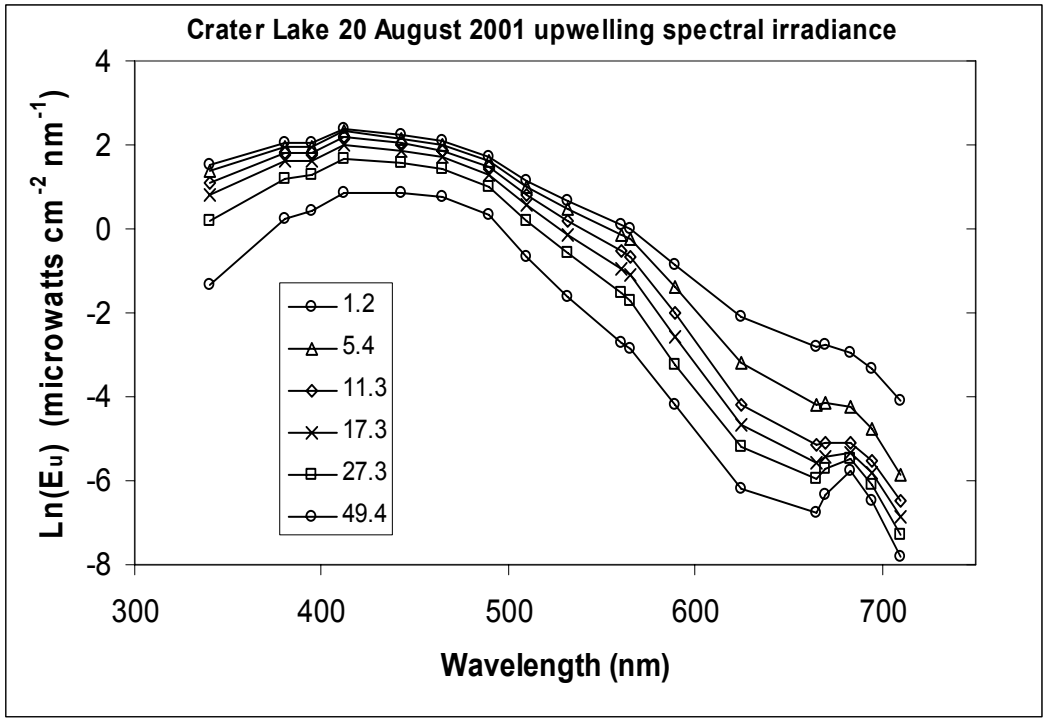

Figure 2B.

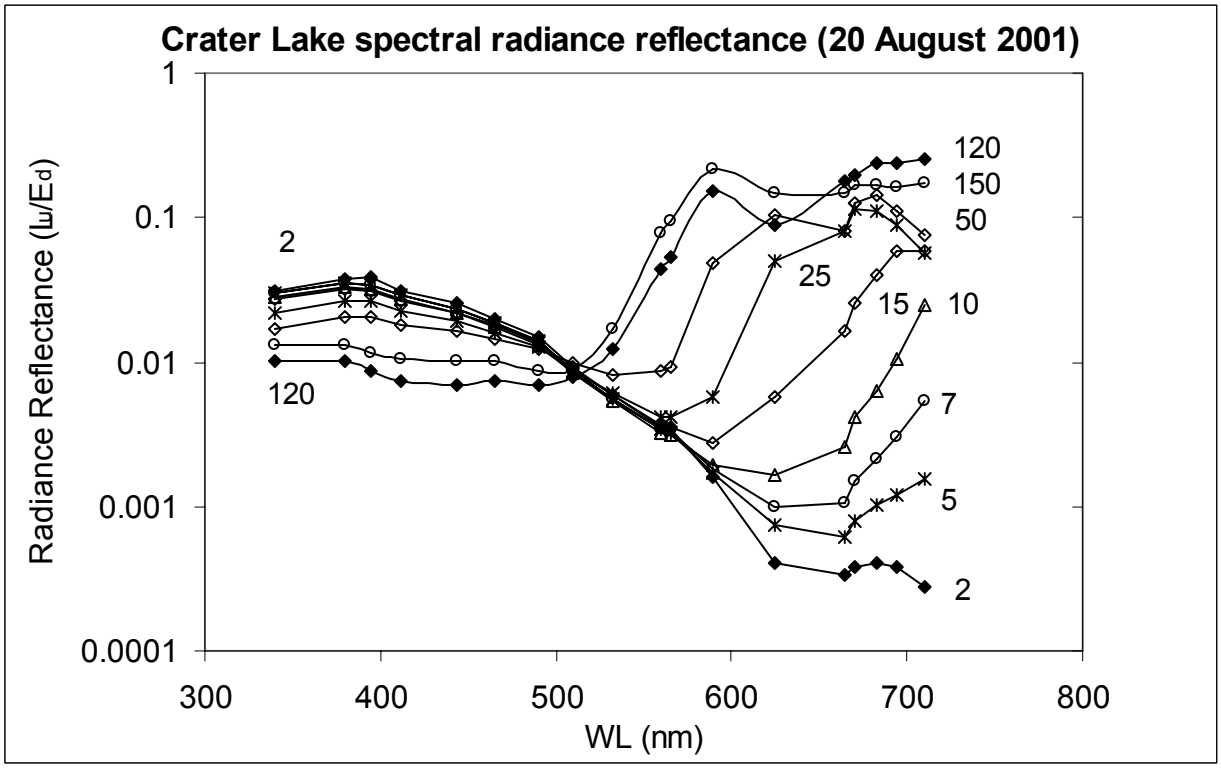

Figure 3.

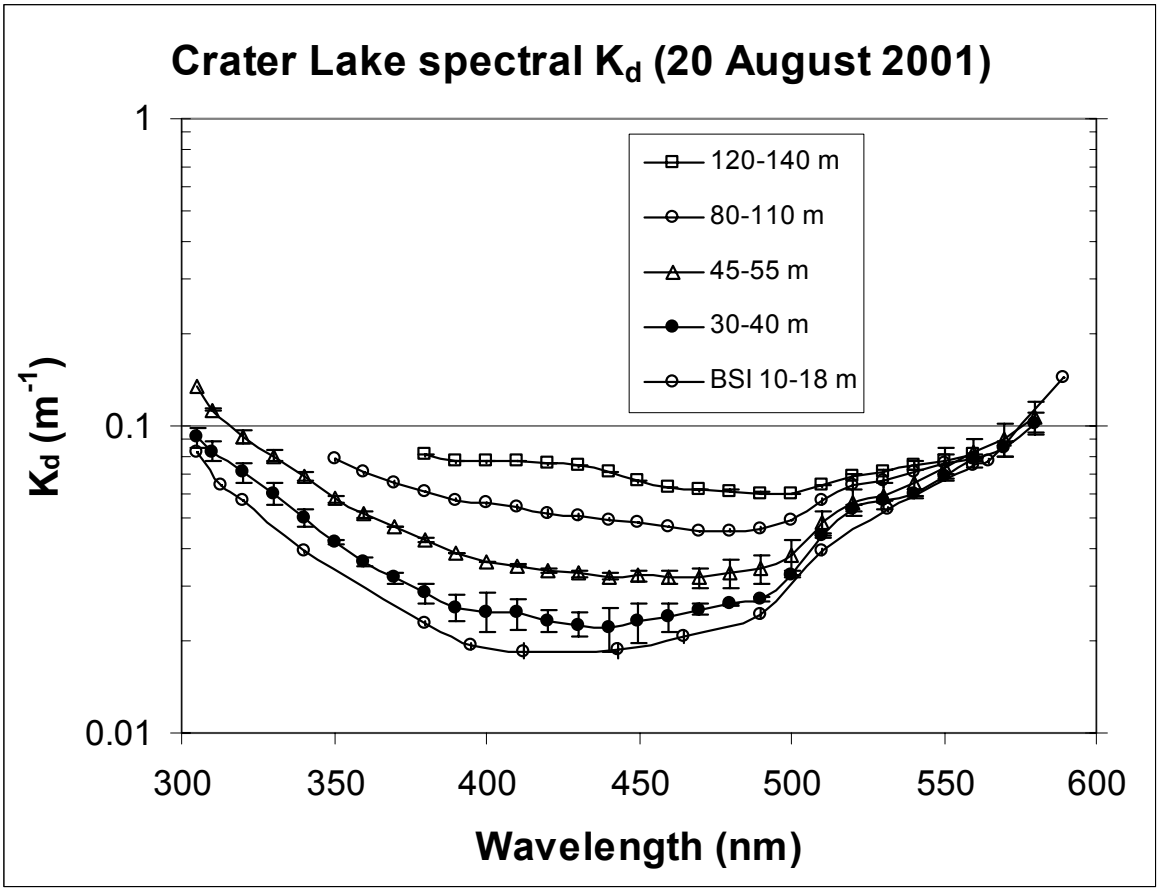
Crater Lake spectral K_d (20 August 2001)
1
0.1
0.01
K_d (m^{-1})
300
350
400
450
500
550
600
Wavelength (nm)
120-140 m
80-110 m
45-55 m
30-40 m
BSI 10-18 m

Figure 4.

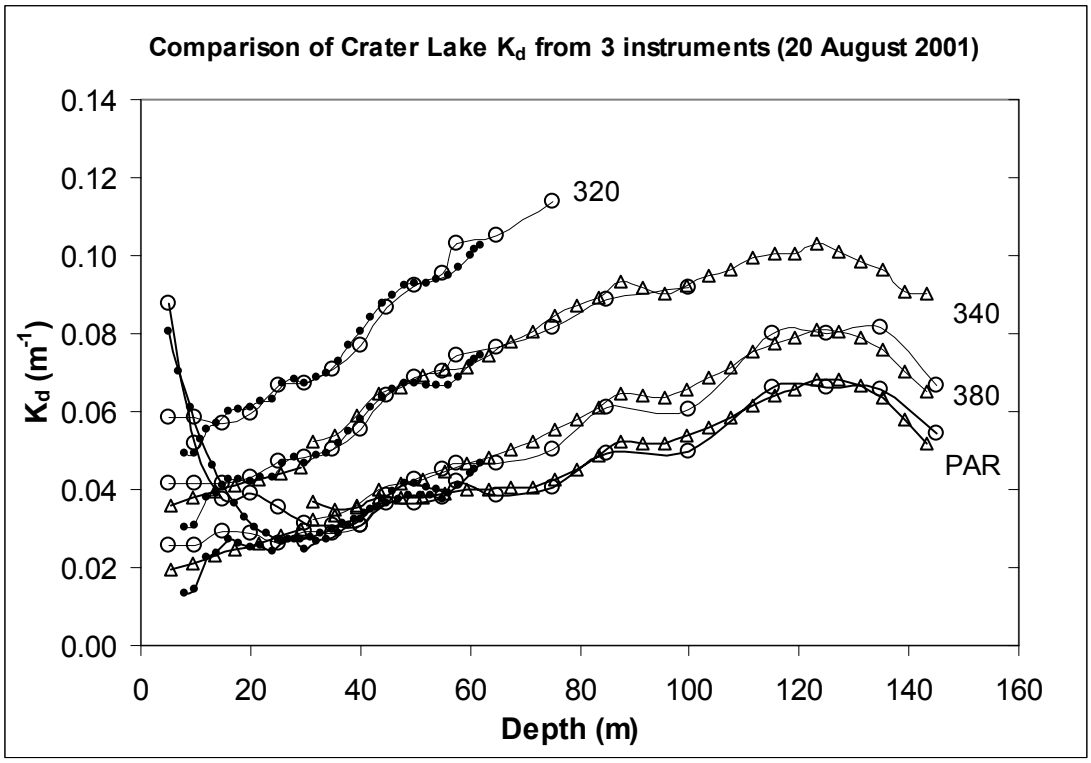
Comparison of Crater Lake K_d from 3 instruments (20 August 2001)
K_d (m^{-1})
0.14
0.12
0.10
0.08
0.06
0.04
0.02
0.00
0
20
40
60
80
100
120
140
160
Depth (m)
320
340
380
PAR

Figure 5.

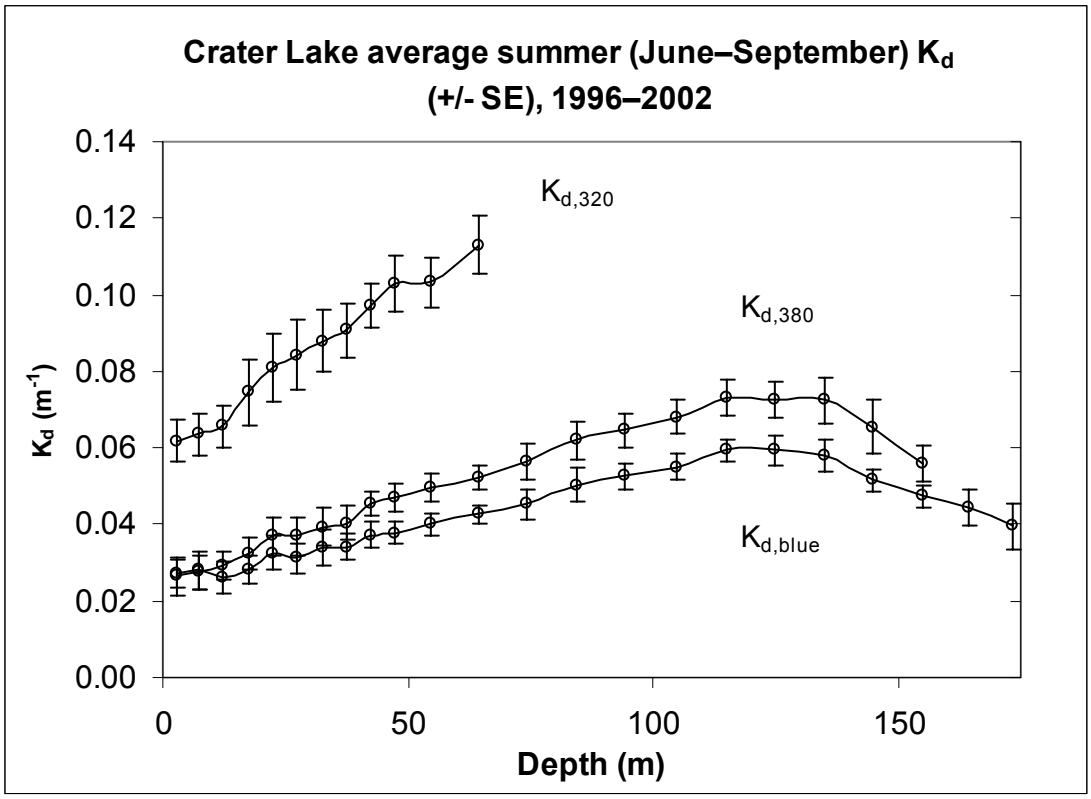
Crater Lake average summer (June–September) K_d (+/- SE), 1996–2002
0.14
0.12
0.10
0.08
0.06
0.04
0.02
0.00
K_d (m^{-1})
$K_{d,320}$
$K_{d,380}$
$K_{d,blue}$
0
50
100
150
Depth (m)

Figure 6.

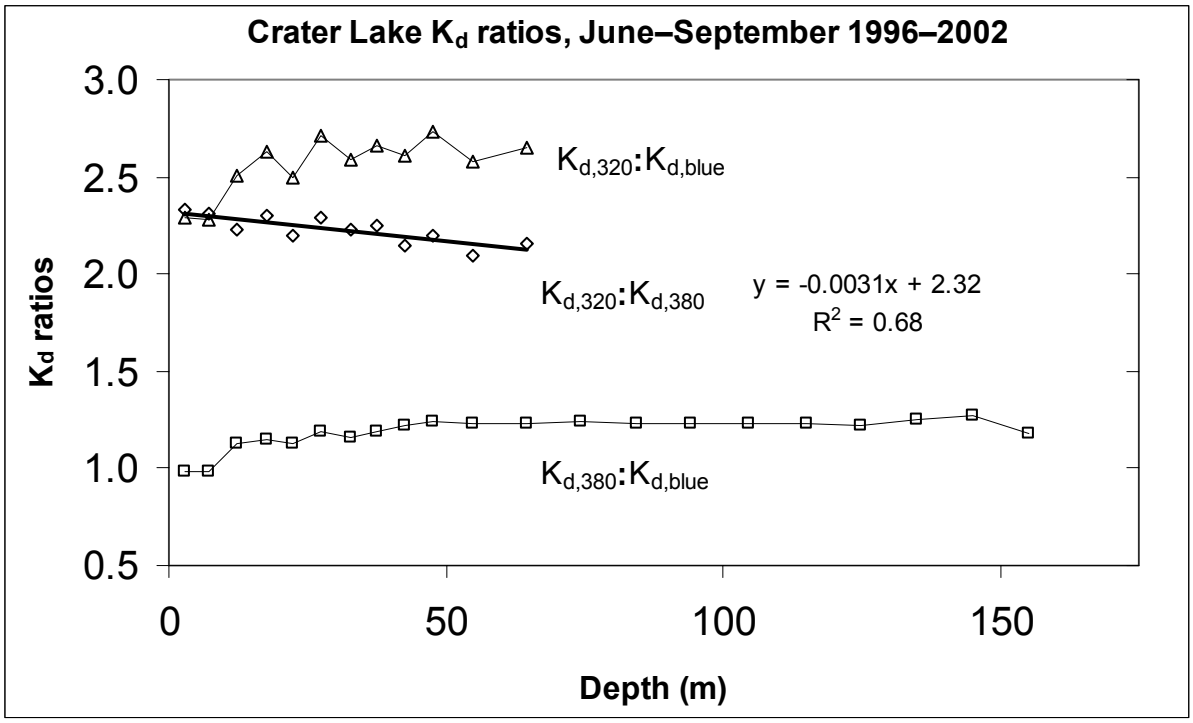
Crater Lake K_d ratios, June–September 1996–2002
3.0
2.5
2.0
1.5
1.0
0.5
K_d ratios
0
50
100
150
Depth (m)
$K_{d,320}$:$K_{d,blue}$
$K_{d,320}$:$K_{d,380}$
y = -0.0031x + 2.32
R^2 = 0.68
$K_{d,380}$:$K_{d,blue}$

Figure 7A.

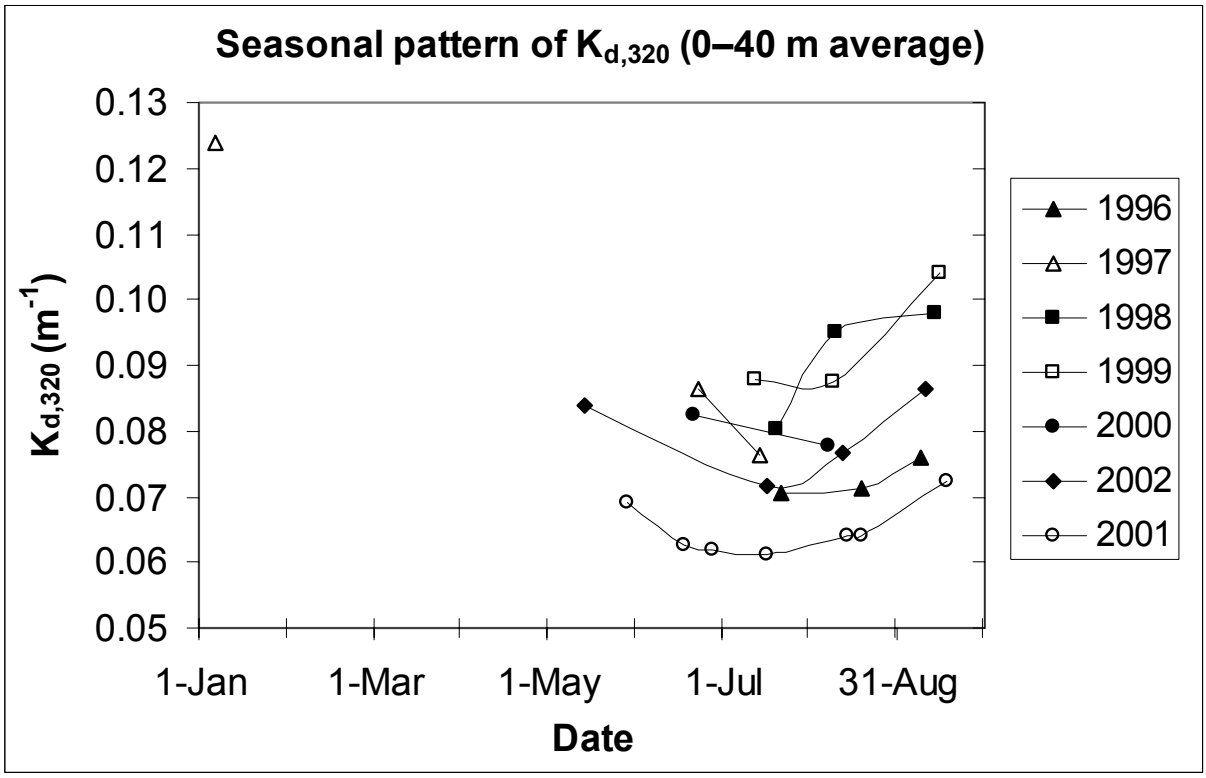

Figurer 7B.

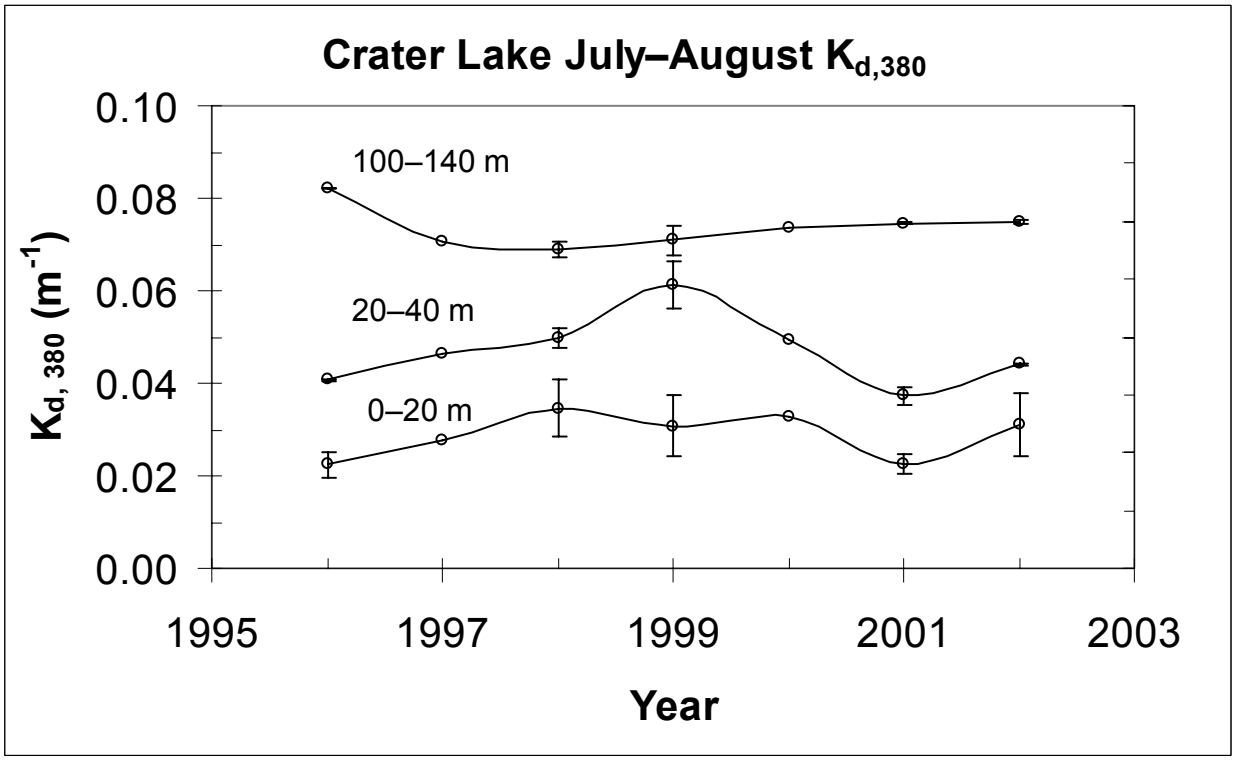

Figure 8A.

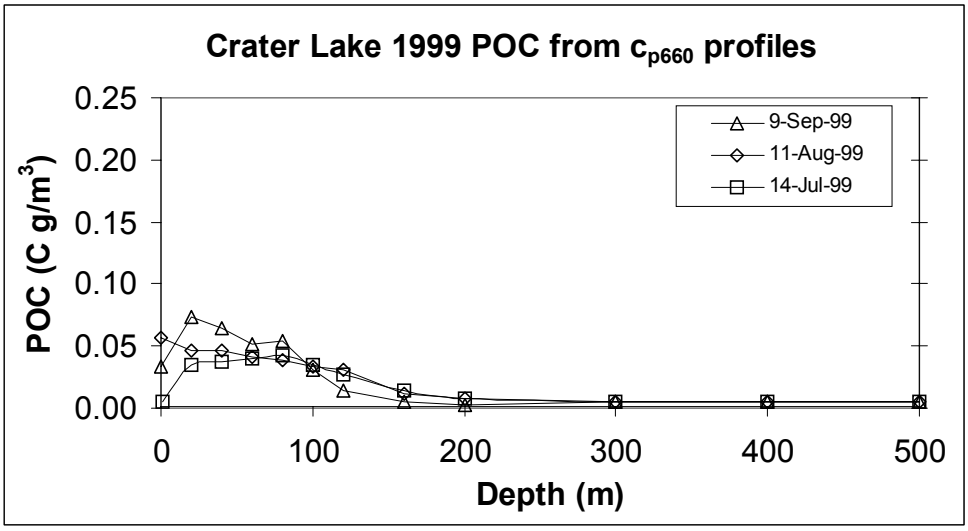

Figure 8B.

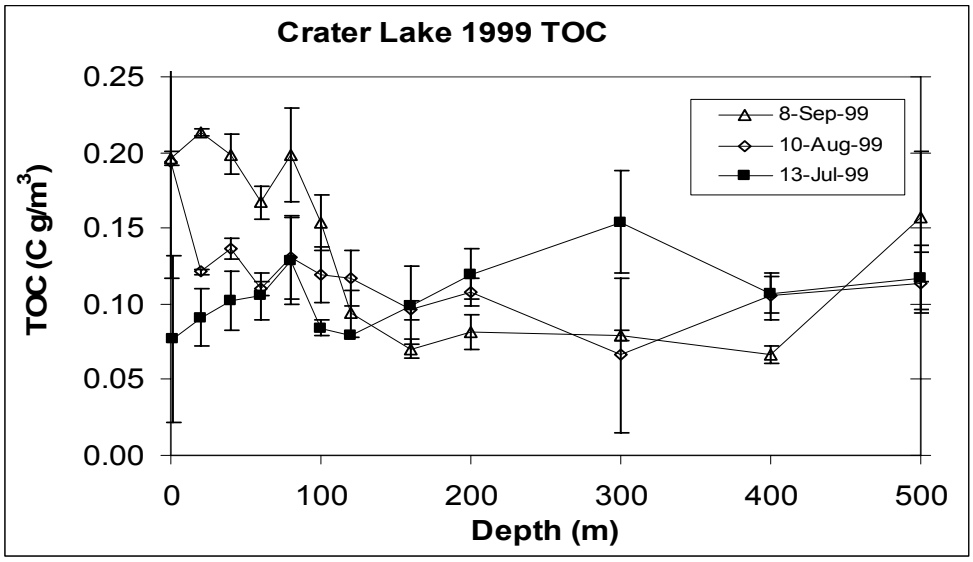

Figure 8C.

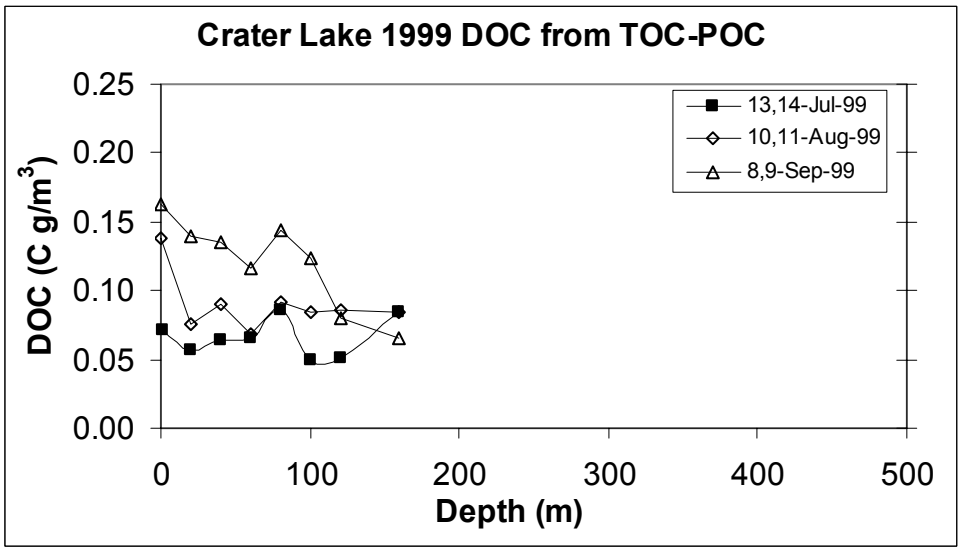

Figure 9A.

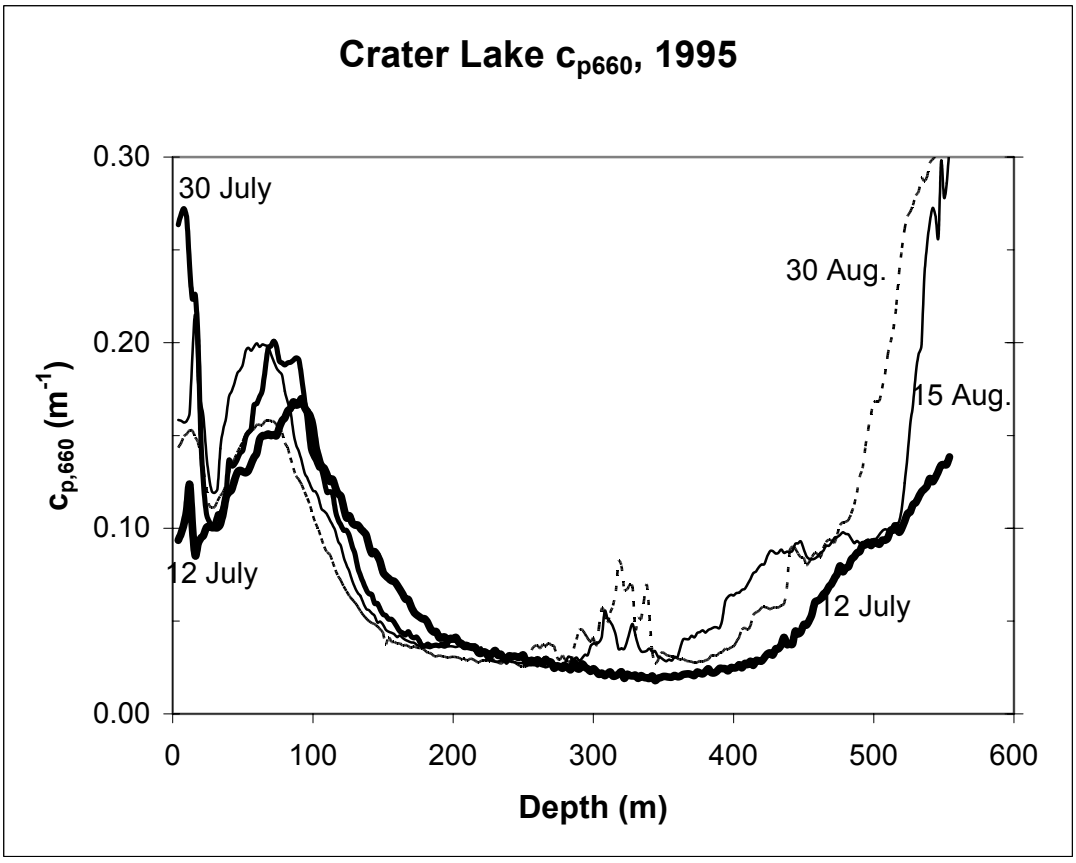

Figure 9B.

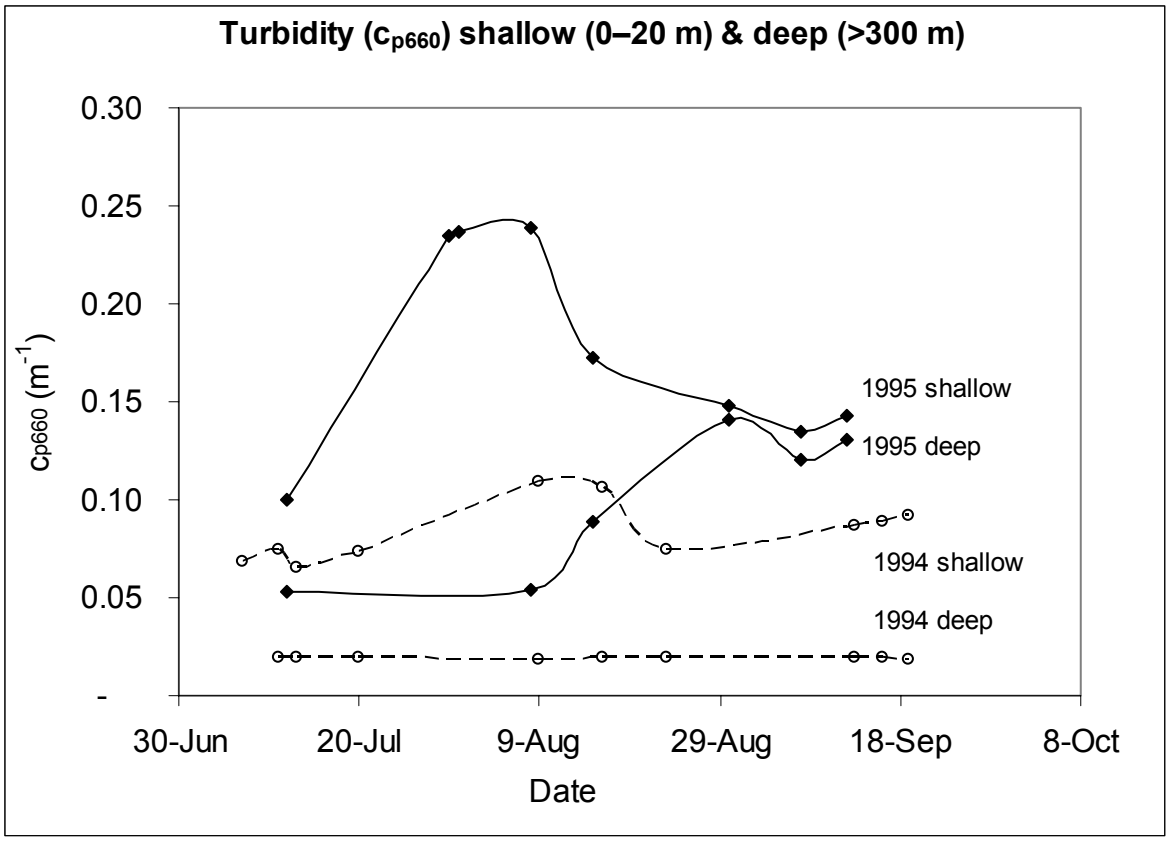

Figure 10A.

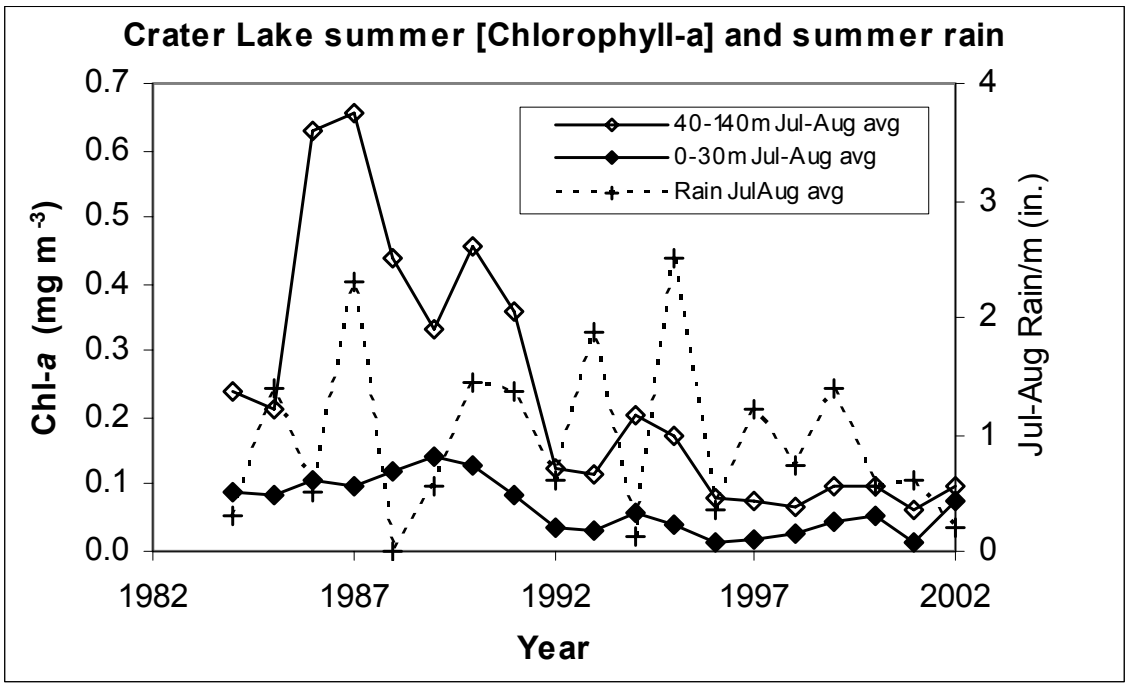

Figure 10B.

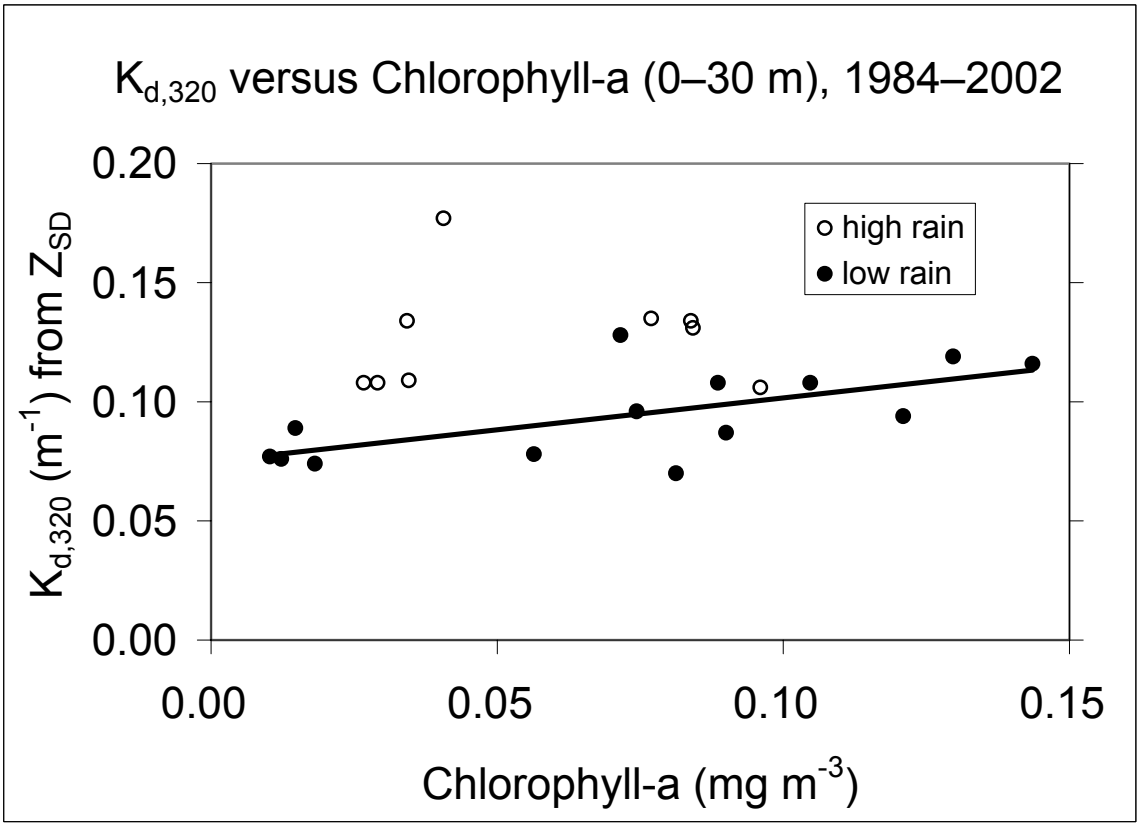

Figure 11A.

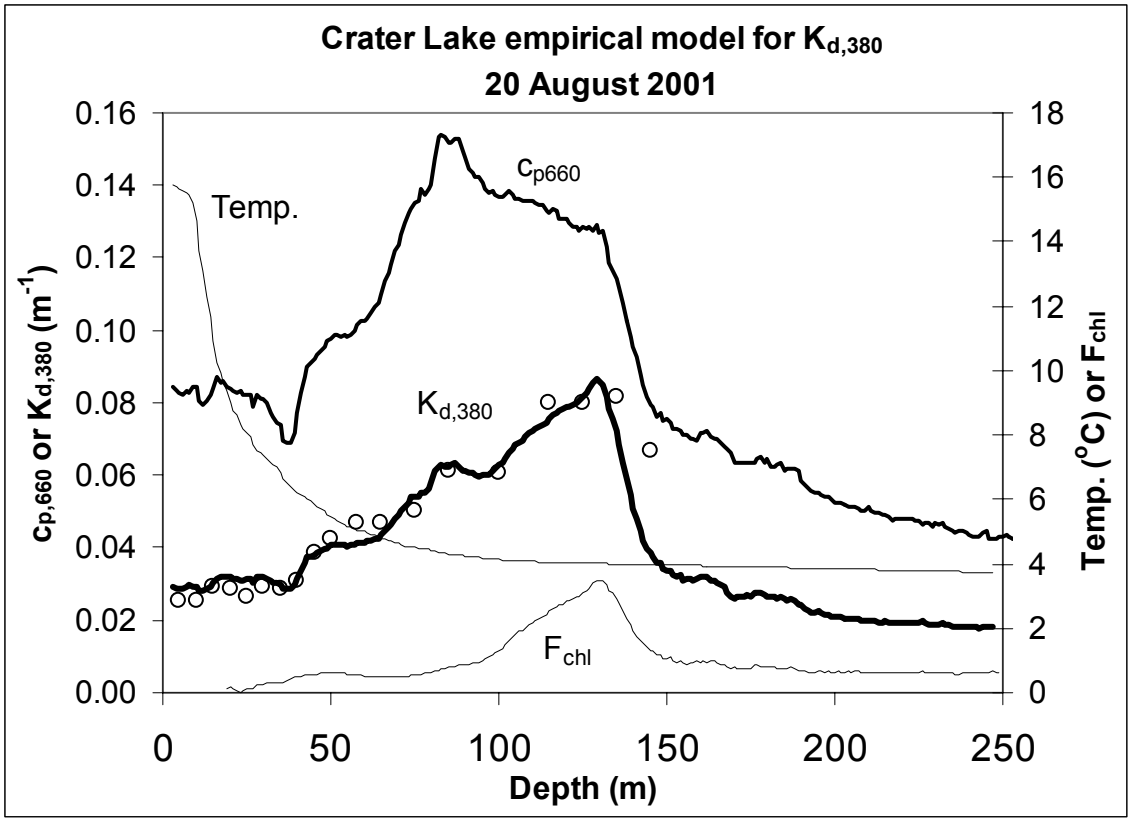

Figure 11B.

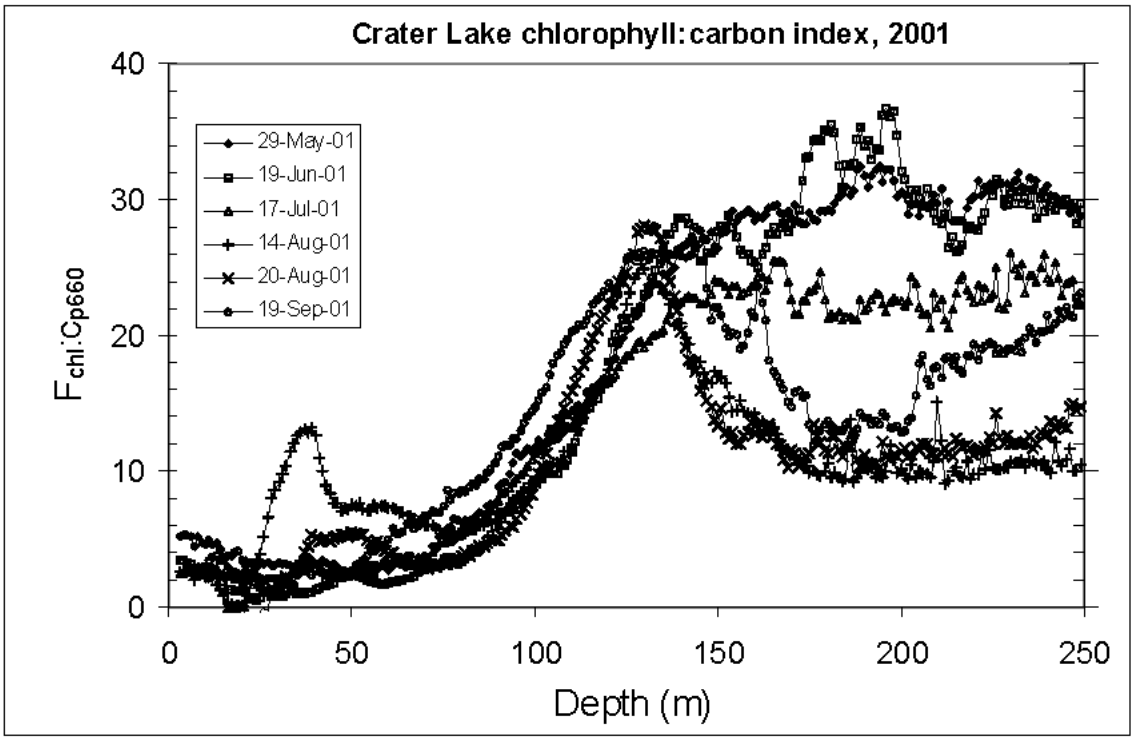

Figure 12A.

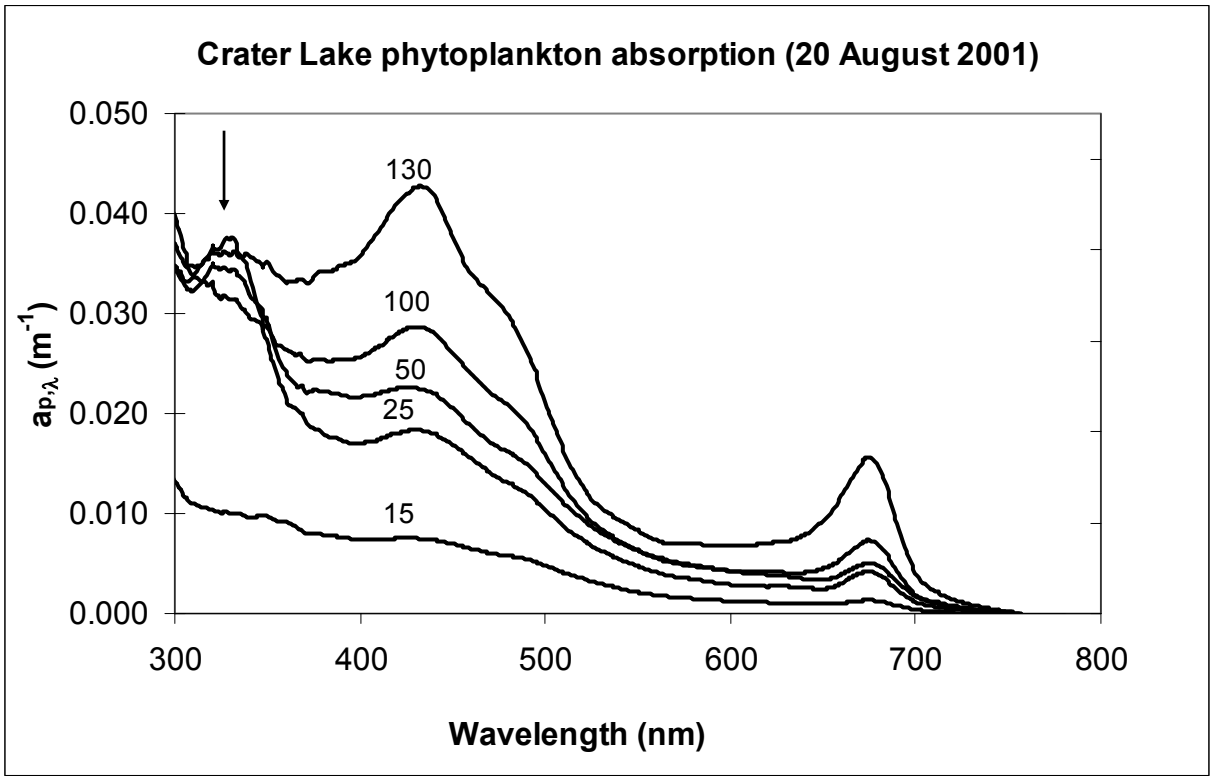

Figure 12B.

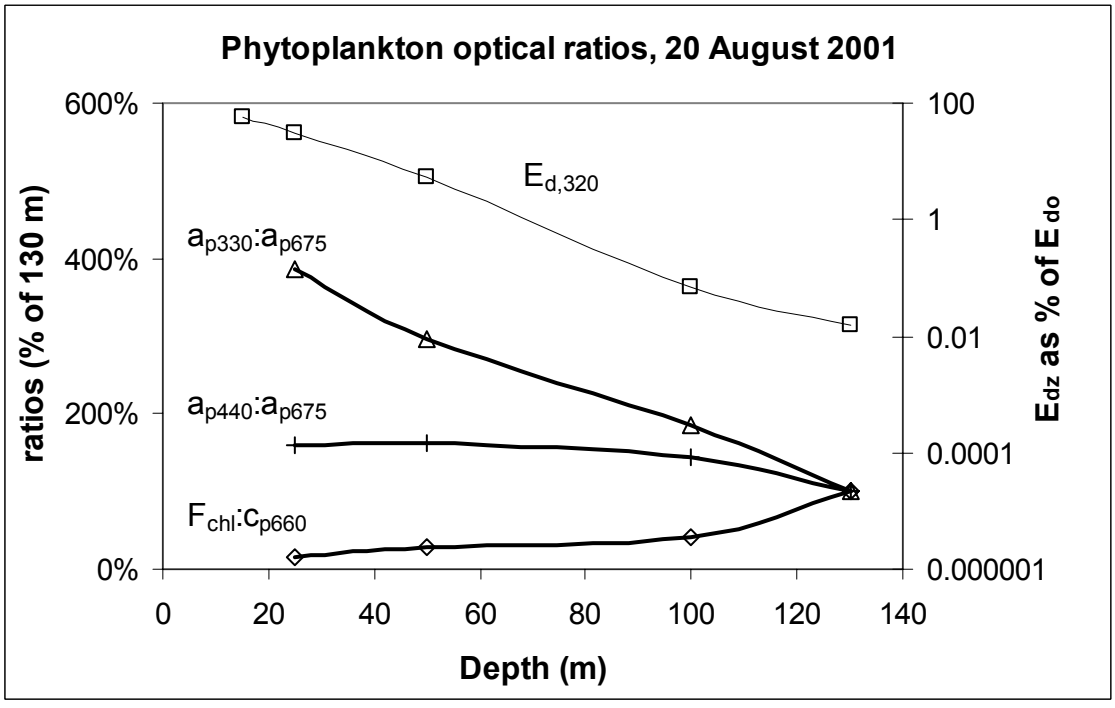

Figure 13A.

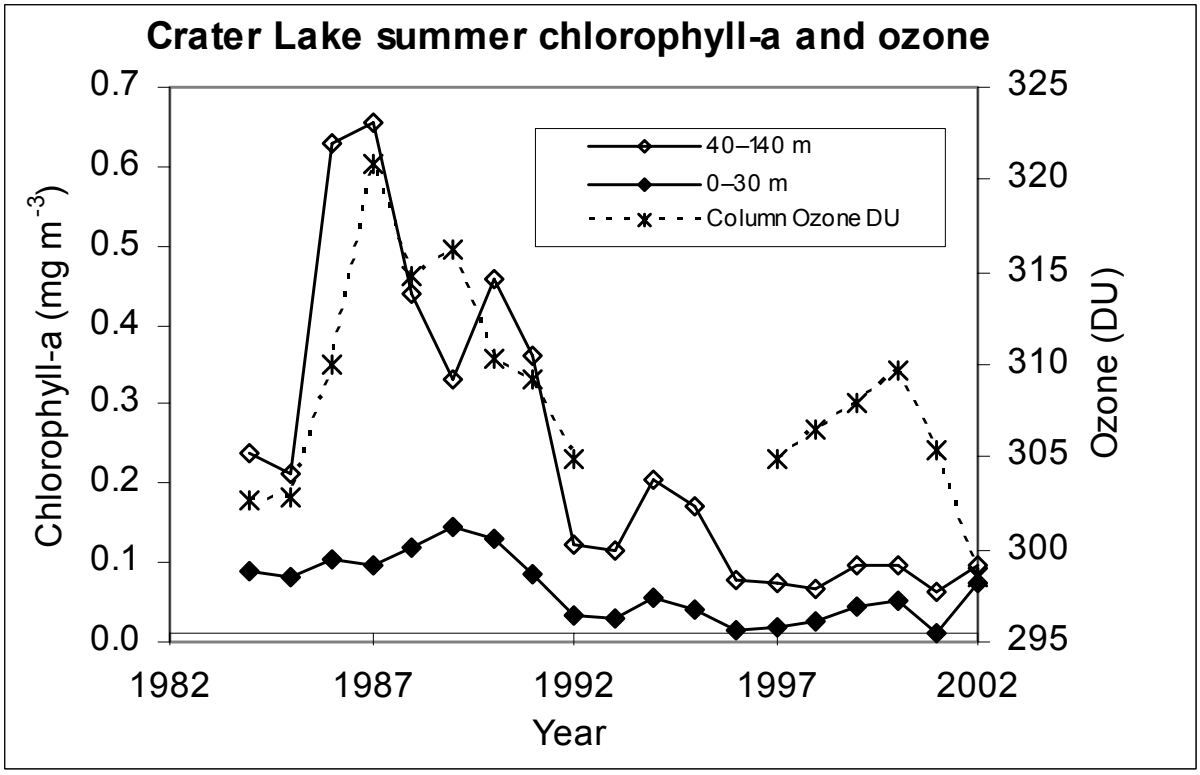

Figure 13B.

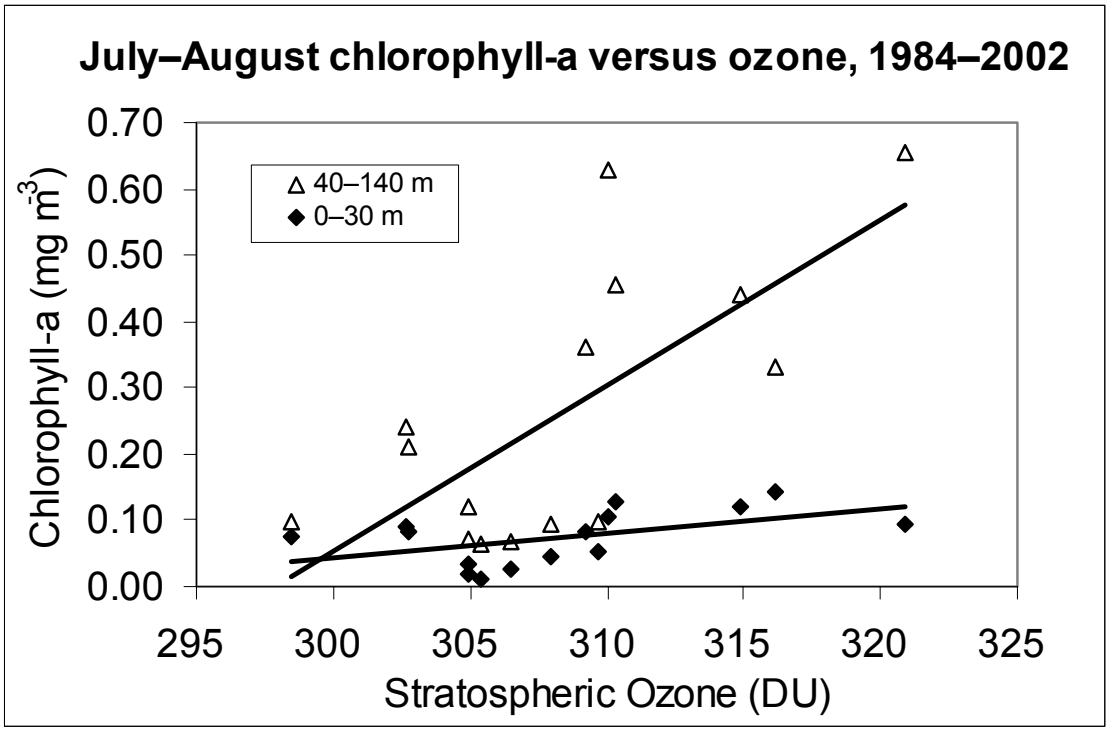

Figure 14A.

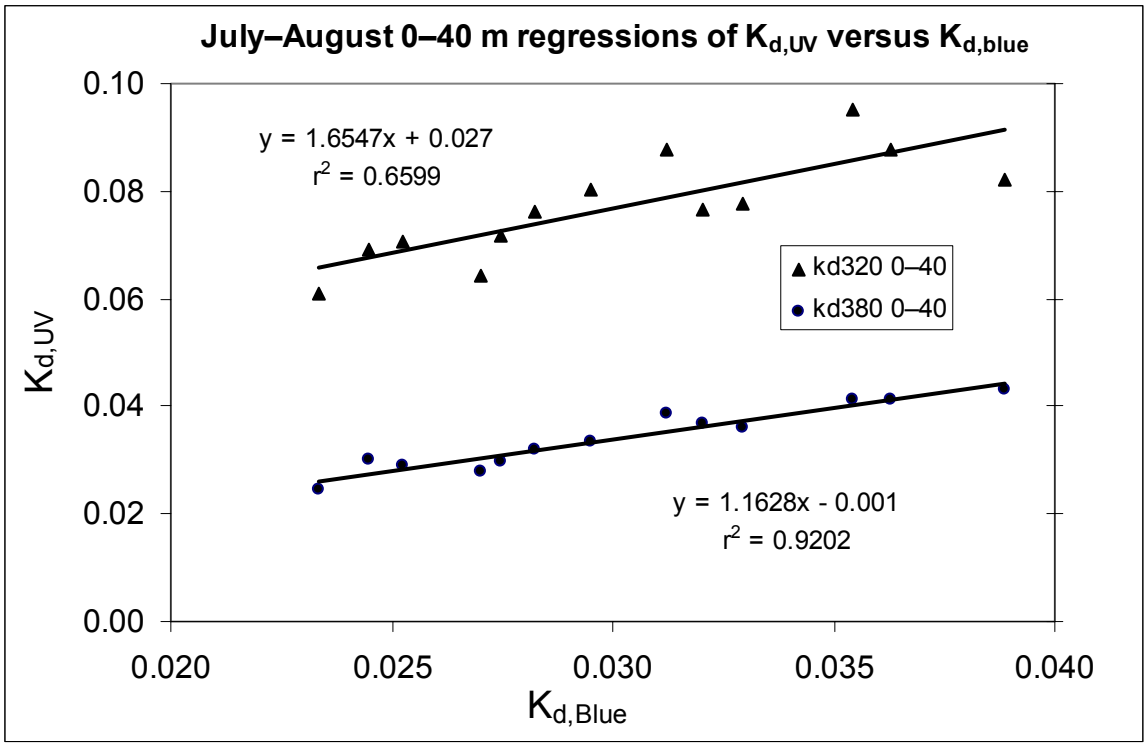

Figure14B.

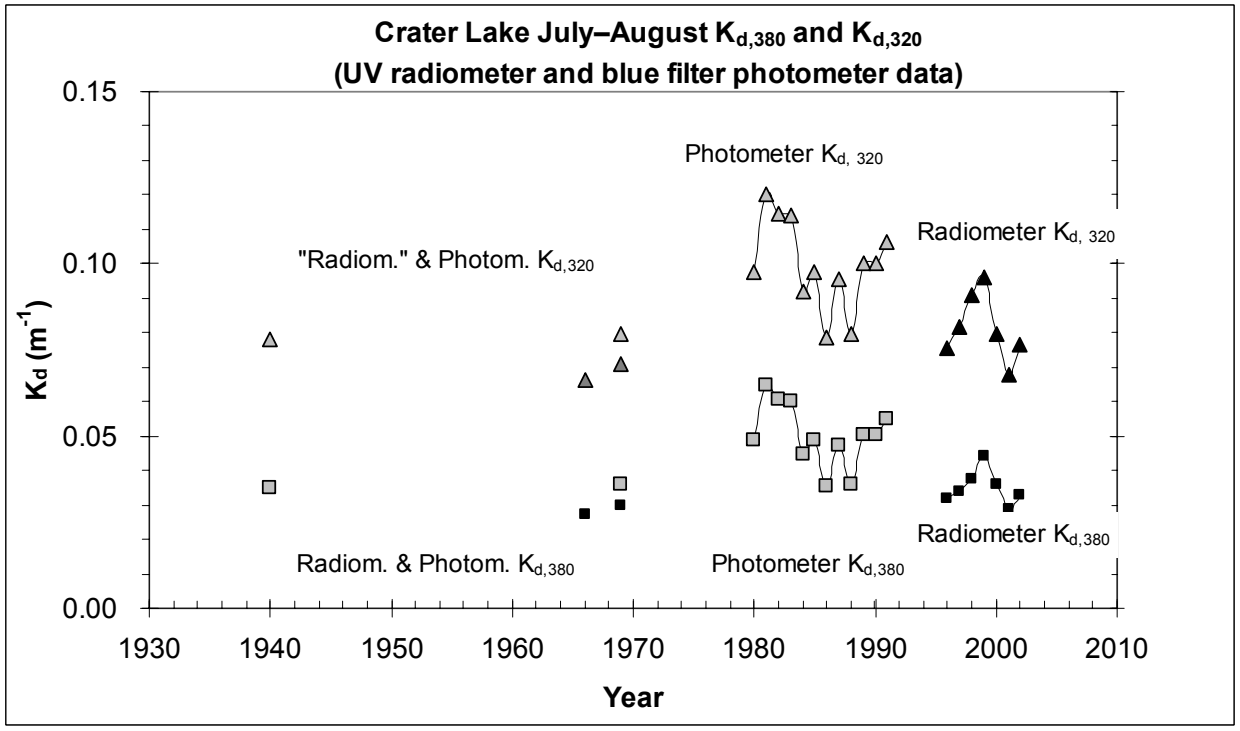

Figure 15A.

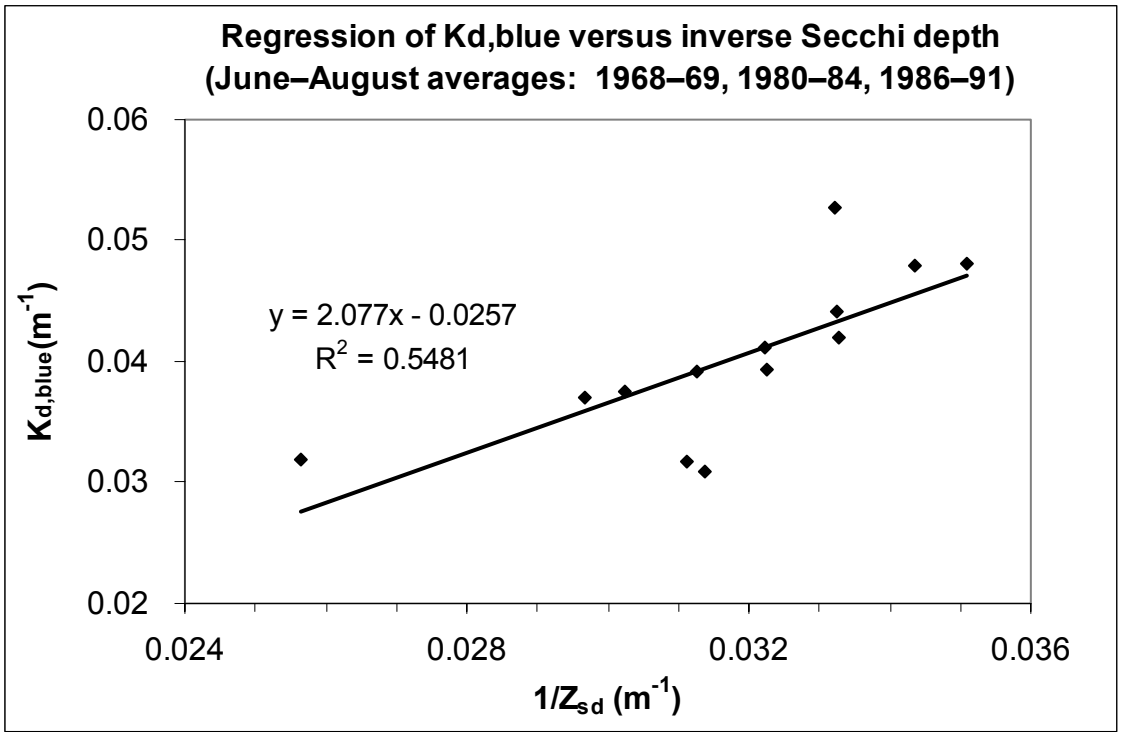

Figure 15B.

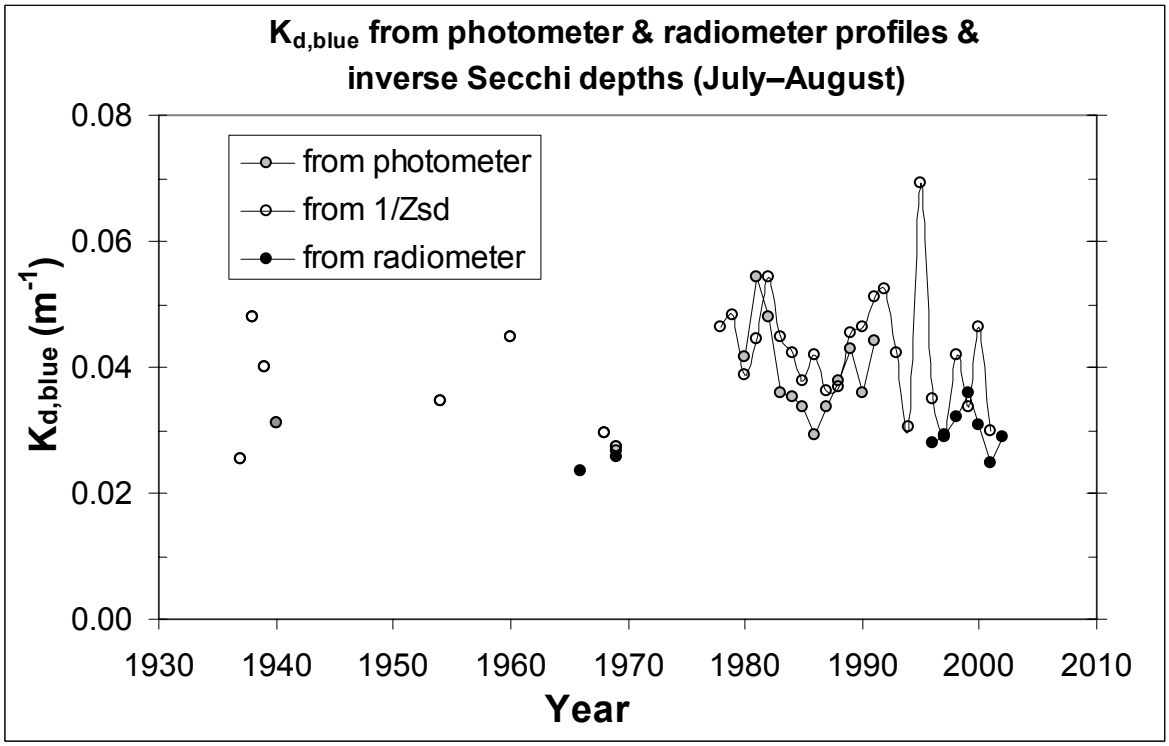

Figure 16A.

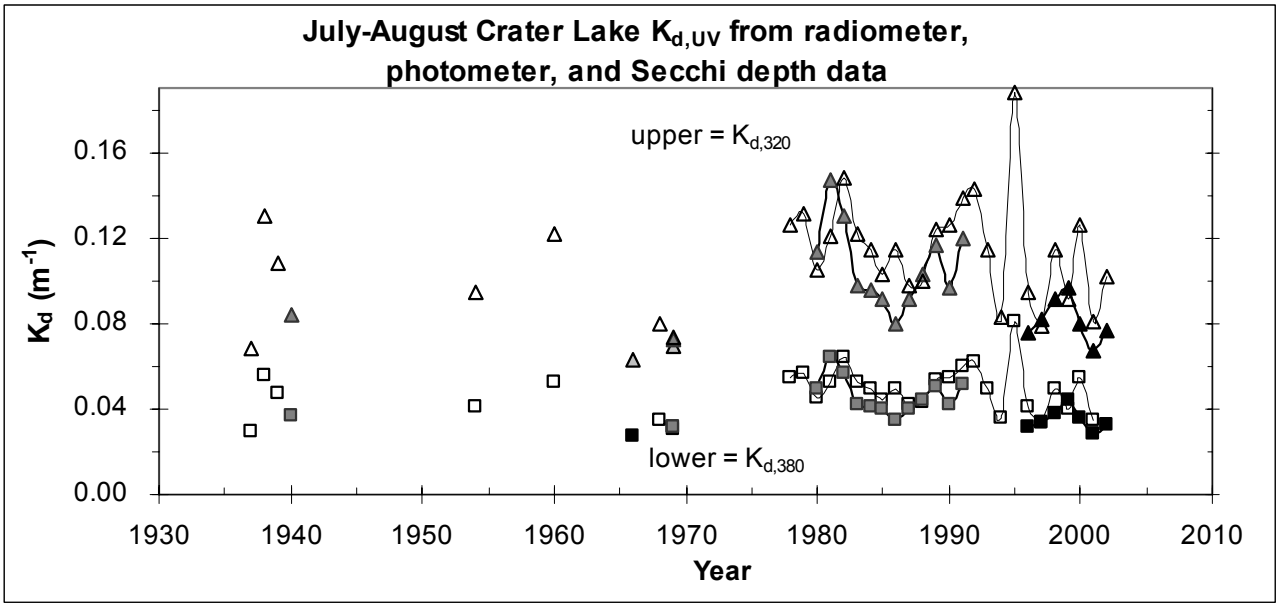

16B.